


## PUBLISHED VERSION

Dorothy Turner, Kenneth Clarke, Davina White & Megan Lewis  
**Mapping areas of Great Artesian Basin diffuse discharge**

This work is licensed under the Creative Commons Attribution 4.0 International License.

### PERMISSIONS

<http://creativecommons.org/licenses/by/4.0/>



**Attribution 4.0 International (CC BY 4.0)**


This is a human-readable summary of (and not a substitute for) the [license](#). [Disclaimer](#).


**You are free to:**

- Share** — copy and redistribute the material in any medium or format
- Adapt** — remix, transform, and build upon the material for any purpose, even commercially.

The licensor cannot revoke these freedoms as long as you follow the license terms.

**Under the following terms:**

-  **Attribution** — You must give [appropriate credit](#), provide a link to the license, and [indicate if changes were made](#). You may do so in any reasonable manner, but not in any way that suggests the licensor endorses you or your use.
- No additional restrictions** — You may not apply legal terms or [technological measures](#) that legally restrict others from doing anything the license permits.



23 June 2017

<http://hdl.handle.net/2440/106110>

# Lake Eyre Basin Springs Assessment

## Mapping areas of Great Artesian Basin diffuse discharge

Prepared for

The Department of Environment, Water and Natural Resources

By

Dorothy Turner, Kenneth Clarke, Davina White & Megan Lewis

School of Biological Sciences

The University of Adelaide

Adelaide, 5005

Final Report August 2015



**Government of South Australia**  
Department of Environment,  
Water and Natural Resources



Department of Environment, Water and Natural Resources

GPO Box 1047, Adelaide SA 5001

Telephone National (08) 8463 6946

International +61 8 8463 6946

Fax National (08) 8463 6999

International +61 8 8463 6999

Website [www.environment.sa.gov.au](http://www.environment.sa.gov.au)

### **Disclaimer**

The Department of Environment, Water and Natural Resources and its employees do not warrant or make any representation regarding the use, or results of the use, of the information contained herein as regards to its correctness, accuracy, reliability, currency or otherwise. The Department of Environment, Water and Natural Resources and its employees expressly disclaims all liability or responsibility to any person using the information or advice. Information contained in this document is correct at the time of writing.



This work is licensed under the Creative Commons Attribution 4.0 International License.

To view a copy of this license, visit <http://creativecommons.org/licenses/by/4.0/>.

**ISBN** 978-1-925369-40-3

### **Preferred way to cite this publication**

Turner D, Clarke K, White D and Lewis M, 2015, *Mapping areas of Great Artesian Basin diffuse discharge*, DEWNR Technical report 2015/55, report by the University of Adelaide to the Government of South Australia, through Department of Environment, Water and Natural Resources, Adelaide

Download this document at: <http://www.waterconnect.sa.gov.au>

## Acknowledgements

The Lake Eyre Basin Springs Assessment (LEBSA) project received valuable guidance from the project Technical Reference Committee members made up of members from various offices, departments and groups and of diverse backgrounds, including the Department of Environment (DE), Bureau of Meteorology (BoM), Geoscience Australia (GA), Queensland Department of Science, Information Technology, Innovation, and the Arts (DSITIA), the SAAL NRM Board and the South Australian Department of Environment, Water and Natural Resources (DEWNR).

The LEBSA project has been delivered concurrently and in-conjunction with an equivalent project run by DSITIA, of which Keryn Oude-egberink (DSITIA LEBSA PM) has been instrumental in providing feedback to the TRC and SA LEBSA project, and guidance to the many DSITIA staff working on the project.

Overarching program guidance and coordination of SA and Qld LEBSA projects was provided by the Executive Steering Committee members: Peter Baker (DE), Edwina Johnson (DE), Anisa Coric (DE), Kriton Glenn (GA), Tim Evans (GA), Phil Deamer (BoM), Sarah van Rooyen (BoM), Brendan Moran (BoM), Tom Carrangis (DEWNR), Tim Ryan (DSITIA) and Keryn Oude-egberink (DSITIA).

The DEWNR LEBSA project team comprised: Andy Harrison (Project Manager), sub-Project Manager (Danny Brock), Travis Gotch, Ronald Bonifacio, Mel White, Dan Wohling, Mark Keppel, Dave Armstrong, Glen Scholz, Matt Miles, (DEWNR), with Catherine Miles (Miles Environmental Consulting) and Katie Fels (Jacobs).

## Summary

The purpose of this report was to develop a method for mapping areas of Great Artesian Basin (GAB) diffuse discharge. These areas of diffuse discharge have two physical expressions amenable to remote sensing: a surface crust of evaporite minerals, and a lower-than-ambient temperature. The evaporite crust is a result of salt buildup as water seeps from the GAB and evaporates at the surface, and the lower-than-ambient temperature is a result of the cooling effect of the evaporation at the soil surface.

We used imagery from the newly launched Landsat 8 satellite, available for free download from the USGS website. Despite the fact that the revisit rate of Landsat is every 16 days, it was challenging to find cloud free imagery which suited our purpose. This was made more difficult by the fact that the study area includes part of four separate Landsat scenes. Ideally, we were looking for a set of cloud-free images a month or two following rain (but dry close to the image date), to allow for a green flush of vegetation, and a second set of images at the end of a dry spell.

We initially investigated combining both the winter and summer Landsat imagery to identify areas which were consistently bright and/or wet over the entire year. This method produced only moderate results, as the bright soils in the summer imagery made it difficult to distinguish the also bright evaporite mineral crusts. The winter imagery was chosen for final analysis as the flush of green vegetation makes it much easier to distinguish the areas of diffuse discharge from the darker background.

We chose two albedo thresholds based on the first component (PC1) of a principal components analysis (PCA). We used training data from previously mapped diffuse discharge with hyperspectral imagery (Lewis et. al., 2013), as well as areas of potential diffuse discharge digitised by Travis Gotch for this project. The PCA used the optical bands of the winter Landsat imagery (bands 1 to 7). The first threshold (0.85) maps the areas of evaporite crust quite well but also captures the extensive bright mullock heaps from opal mining in the Coober Pedy region, as well as bright sands on the edge of the Simpson Desert and along the course of Peake Creek. Much of the mullock heaps are excluded with the higher albedo threshold of 0.90, but likewise the area of evaporite mapped is less. Further investigation will determine which threshold is most appropriate, depending on the purpose of the exercise. The albedo threshold alone can detect both historic (no longer wet) and current diffuse discharge.

To locate currently active areas of diffuse discharge we developed a temperature threshold. Areas below this temperature are likely to be wet. As the imagery for the study area covered four Landsat paths we had to develop separate thresholds per path/date. We used previously mapped Near Surface Moisture Index data (NSMI) and archival ASTER temperature data (Lewis et. al., 2013), as well as the areas of potential diffuse discharge digitised by Travis Gotch as training data. We had the added difficulty of having no training data for Landsat path 101 and had to make

assumptions based on the other path's threshold values. The separate temperature thresholds per Landsat path were then combined into one layer.

Finally, we combined each of the albedo thresholds (0.85 and 0.90) with the temperature threshold. Results using the combined bright and wet areas were much improved at identifying areas of active diffuse discharge. Our results were evaluated using a subset of the Lewis and Gotch data.

The methodology presented here uses free satellite data, and could in principle be applied elsewhere to detect similar diffuse discharge zones. However, variation in soil colour or spring geomorphology would make accuracy assessment advisable if applied elsewhere.

As there is greater contrast between areas of evaporite and exposed bright soils in winter, we recommend that winter imagery be used for future analysis.

## Table of Contents

<b>Acknowledgements .....</b>	<b>iii</b>
<b>Summary.....</b>	<b>iv</b>
<b>Table of Contents .....</b>	<b>vi</b>
<b>Figures.....</b>	<b>vii</b>
<b>Tables .....</b>	<b>viii</b>
<b>1 Introduction.....</b>	<b>1</b>
<b>2 Methods.....</b>	<b>3</b>
2.1 Study area.....	3
2.2 Satellite image data .....	3
2.3 Satellite image pre-processing .....	8
2.4 Training and evaluation data.....	10
2.4.1 Lewis data .....	10
2.4.2 Gotch diffuse discharge data.....	11
2.4.3 Gotch spring vent data .....	11
2.5 Evaporite mineral detection – Historical and current discharge .....	17
2.6 Wet ground detection – Current discharge .....	17
2.7 Combined evaporite mineral and wet ground detection .....	18
2.8 Accuracy evaluations .....	18
<b>3 Results .....</b>	<b>20</b>
3.1 Evaporite mineral detection – Historical and current discharge .....	20
3.2 Wet ground detection – Current discharge .....	28
3.3 Combined evaporite mineral and wet ground detection .....	34
3.4 Accuracy evaluations .....	34
3.4.1 Albedo thresholds .....	35
3.4.2 Temperature thresholds.....	40
3.4.3 Combined albedo and temperature thresholds.....	40
3.4.4 Gotch spring vent data .....	40
<b>4 Discussion and recommendations.....</b>	<b>45</b>
4.1 Recommendations.....	46
<b>References .....</b>	<b>47</b>
<b>Appendix 1. Monthly rainfall at Coober Pedy Airport 2013 and 2014 (mm) ...</b>	<b>48</b>
<b>Appendix 2. Enlargements of areas of interest .....</b>	<b>50</b>

## Figures

Figure 1: Study area.....	4
Figure 2: Analysis mask covering the study area, Francis Swamp, Freeling South and the Hermit Hill Complex for both the (a) winter and (b) summer mosaicked Landsat imagery .....	9
Figure 3: Freeling South Lewis data (a) diffuse discharge 2011 (b) near surface moisture 2011.....	13
Figure 4: Francis Swamp Lewis data (a) ASTER temperature 2001 (b) near surface moisture 2009..	14
Figure 5: Hermit Hill Complex Lewis data (a) diffuse discharge 2009 and 2011 (b) near surface moisture 2009 (c) near surface moisture 2011 .....	15
Figure 6: (a) Gotch potential diffuse discharge areas divided into training and evaluation data (b) Gotch springs data.....	16
Figure 7: Winter and summer Landsat true colour images (red: band 4; green: band3; blue: band 2) for the Hermit Hill Complex and the Gotch potential diffuse discharge training areas .....	21
Figure 8: Principal Component 1 of combined OLI bands summer, winter and combined summer and winter mosaics (a) entire analysis area (b) Hermit Hill Complex (c) subset of training Gotch potential diffuse discharge areas .....	22
Figure 9: Mullock heaps from opal mining along the A87 outside Coober Pedy which have a very high albedo and a lower temperature than the surrounding red soil landscape .....	24
Figure 10: Hermit Hill winter Principal Component 1 thresholds for diffuse discharge (a) Hermit Hill Complex road network and Lewis diffuse discharge data (b) PC1 0.80 threshold (c) PC1 0.85 threshold (d) PC1 0.90 threshold.....	25
Figure 11: Principal Component 1 (PC1) diffuse discharge thresholds for the Gotch training areas (a) PC1 0.85 threshold (b) PC1 0.90 threshold.....	26
Figure 12: Principal Component 1 (PC1) diffuse discharge thresholds for the analysis area (a) PC1 0.85 threshold (b) PC1 0.90 threshold.....	27
Figure 13: Band 10 temperature (a) winter temperature mosaicked per Landsat path (b) summer temperature mosaicked per Landsat path .....	29
Figure 14: Hermit Hill winter temperature thresholds (Path 099) (a) Hermit Hill Complex and Lewis NSMI data (b) 17.43 °C threshold (c) 16.05 °C threshold (d) 16 °C threshold .....	30
Figure 15: Temperature threshold for the Gotch training areas (a) winter temperatures and training polygons (b) temperature threshold of 13.5 degrees Celsius .....	31
Figure 16: Temperature thresholds for the analysis area: Path 099 = 16 °C; Path 100 = 13.5 °C; Path 101 = 19.5 °C .....	32
Figure 17: Combined PC1 albedo and temperature thresholds for the analysis area: (a) PC1 threshold of 0.85 + combined Landsat path temperature thresholds (b) PC1 threshold of 0.90 + combined Landsat path temperature thresholds.....	33
Figure 18: Comparison of Lewis diffuse discharge evaluation data with PC1 albedo thresholds 0.85 and 0.90 (a) Freeling South 2011 (b) Hermit Hill Group 2011 (c) West Finniss Group 2011 .....	39
Figure 19: Comparison of Lewis NSMI and ASTER Temperature evaluation data with temperature thresholds (a) Freeling South NSMI 2011 (b) Hermit Hill Complex NSMI 2011 (c) Francis Swamp NSMI 2009 (d) Francis Swamp ASTER Temperature 2001.....	42



## Tables

Table 1: Landsat 8 Operational Land Imager (OLI) and Thermal Infrared Sensor (TIRS) .....	5
Table 2: Dates of Landsat 8 OLI TIRS L1T imagery (path/row) and % cloud cover .....	6
Table 3: Coober Pedy airport monthly rainfall (mm) .....	7
Table 4: The Lewis datasets .....	10
Table 5: Training and evaluation datasets .....	12
Table 6: Zonal statistics of winter and summer Principal Component 1 (PC1) for the Lewis and Gotch diffuse discharge training datasets .....	23
Table 7: Statistics of band 10 temperature (degrees Celsius) for each Landsat 8 path for winter and summer images .....	28
Table 8: Areas mapped by thresholds and their combinations .....	34
Table 9: Data used in evaluation of diffuse discharge mapping .....	37
Table 10: Comparison of the area (hectares) of both the training and evaluation data with the area of mapped diffuse discharge in the same vicinity .....	38
Table 11: Percentage of vents within a range of distances from areas of diffuse discharge mapped by the albedo and temperature thresholds and their combinations .....	43
Table 12: Percentage of vents per flow attribute within a range of distances from areas of diffuse discharge mapped by the albedo and temperature thresholds and their combinations for the GAB Springs RTK vents .....	43

## 1 Introduction

This report is part of a series of studies forming part of the Lake Eyre Basin Springs Assessment (LEBSA) project. The LEBSA project is one of three water knowledge projects undertaken by the South Australian Department of Water, Environment and Natural Resources (DEWNR) to inform the Bioregional Assessment Programme in the Lake Eyre Basin (LEB). The three projects are:

- Lake Eyre Basin Rivers Monitoring (LEBRM)
- Arckaringa Basin and Pedirka Basin Groundwater Assessment
- Lake Eyre Basin Springs Assessment (LEBSA).

The Bioregional Assessment Programme is a transparent and accessible programme of baseline assessments that increase the available science for decision making associated with potential water-related impacts of coal seam gas (CSG) and large coal mining (LCM) developments. The coal-bearing Arckaringa, Pedirka, Cooper and Galilee basins have been identified as regions where CSG and LCM developments are likely to occur or increase in the future. Bioregional assessments are being prepared in the LEB for the four coal regions to strengthen the science underpinning future decisions about CSG and LCM activities and their impacts on groundwater quality, surface water resources and aquatic ecosystems.

The objective of the LEBSA project was to address knowledge gaps relating to the potential impacts of mining developments on groundwater resources and assets across the LEB. In particular, the project aimed to characterise and attribute springs and other GDEs that are critical for the maintenance of those assets (e.g. ecological, hydrogeological, hydrochemical), in a way that is consistent across South Australia and Queensland.

For the LEBSA project, the South Australian Department of Environment, Water and Natural Resources (DEWNR) requested a method for mapping and quantifying areas of Great Artesian Basin (GAB) diffuse discharge. The methods required will be dependent on the physical properties of diffuse discharge in the region.

This came about through the National Partnership Agreement on Coal Seam Gas and Large Coal Mining Development (2012). The agreement (between the Commonwealth of Australia, and New South Wales, Victoria, Queensland, South Australia and the Northern Territory) recognises that the signatories have a mutual interest in the long term health, quality and viability of Australia's water resources and the sustainable development of coal seam gas and coal mining industries.

Bioregional assessments (BAs) are one of the key mechanisms to assist the Independent Expert Scientific Committee on Coal Seam Gas and Large Coal Mining Development (the IESC) to provide independent advice to Australian Government and state government regulators on potential water-related impacts of coal seam gas (CSG) and large coal mining development proposals, ensuring it is based on the best available science and independent expert knowledge.

The Lake Eyre Basin (LEB) has been identified as a current area for a bioregional assessment. The Lake Eyre Basin Springs Assessment (LEBSA) project is a critical data acquisition project that will supply up to date scientific baseline data to be used as part of the bioregional assessment for the LEB. The project presented herein (Mapping areas of GAB diffuse discharge) forms part of the LEBSA.

In the region, areas of diffuse discharge occur when water escapes from confining aquifers of the GAB, rises to the surface and then evaporates. As the water evaporates, dissolved salts precipitate and accumulate on the surface as a crust of evaporite minerals, and then, because of the low rainfall, persist for very long periods. Areas of diffuse discharge are distinguished from springs in that the flow from the GAB is low enough, and the evaporation rate is high enough that there is no standing or flowing surface water.

Thus, there are two expressions of active diffuse discharge zones that are amenable to remote sensing:

- the area of evaporite minerals, which is indicative of either current or historical diffuse discharge, and
- the area of near-surface wet soil, which is indicative of current diffuse discharge

These two expressions have previously been successfully mapped with remote sensing methods using hyperspectral imagery at Freeling South, Francis Swamp and the Hermit Hill Complex (White et. al., 2013). In addition satellite thermal imagery has been used to map near-surface moisture at Francis Swamp (White et. al., 2013). It is however noteworthy that inactive diffuse discharge zones, those that are no longer being supplied with water, may still exhibit surface evaporate minerals but no wet soils.

In this report we outline methods for detecting and mapping both expressions of diffuse discharge using Landsat multi spectral imagery, and evaluate the accuracy of the methods and results using the best available independent data on distribution of diffuse discharge.

## 2 Methods

### 2.1 Study area

The study area (Figure 1) covers an area of approximately 18,500 km<sup>2</sup>, stretching from Oodnadatta in the north, to Anna Creek in the south east and Coober Pedy in the south west. It incorporates part or all of almost 30 pastoral leases including Anna Creek, Nilpinna, The Peake, Allandale, Mount Barry, Todmorden and Arckaringa.

The broader area of interest, which includes Freeling South, Francis Swamp and the Hermit Hill Complex (Figure 2), is covered in part by five Landsat scenes ( Path/Row 99/80, 100/79, 100/80, 101/79 and 101/80) (Figure 1). The analysis mask (a subset of these four scenes) is almost 60,000 km<sup>2</sup> (Figure 2).

The area is predominantly situated in the Stony Plains bioregion, which is a gently sloping or undulating erosional plateau, with some low hills. Much of the south east is a gently sloping alluvial plain with extensive dunefields (part of the Simpson Strzelecki Dunefields bioregion).

The area has a desert climate, and experiences mild winters and hot summers, where temperatures often exceed 40 °C. Average annual rainfall is very low, ranging from 100 to 200 mm, but also highly erratic and large rainfall events may occur in any month.

The area supports very little plant growth due to water limitation. The predominant soils are crusty red duplex and much of the vegetation is a mixture of chenopod shrubland with low woodland and some open grassland.

### 2.2 Satellite image data

The following methods use Landsat 8 Operational Land Imager (OLI) and Thermal Infrared Sensor (TIRS) data. This latest Landsat satellite was launched in February 2013 and became operational in May of that year. Scenes are approximately 170 km north-south by 183 km east-west, with a revisit rate of 16 days, and are available free of charge from the United States Geological Survey (USGS) (<http://glovis.usgs.gov/>).

Images consist of nine spectral bands with a spatial resolution of 30 metres for Bands 1 to 7 and 9 (Table 1). The new ultra-blue band (band 1) is useful for coastal and aerosol studies, while the new band 9 is useful for cirrus cloud detection. The resolution for Band 8 (panchromatic) is 15 metres. Thermal bands 10 and 11 are useful in providing more accurate surface temperatures and are collected at 100 metre resolution.

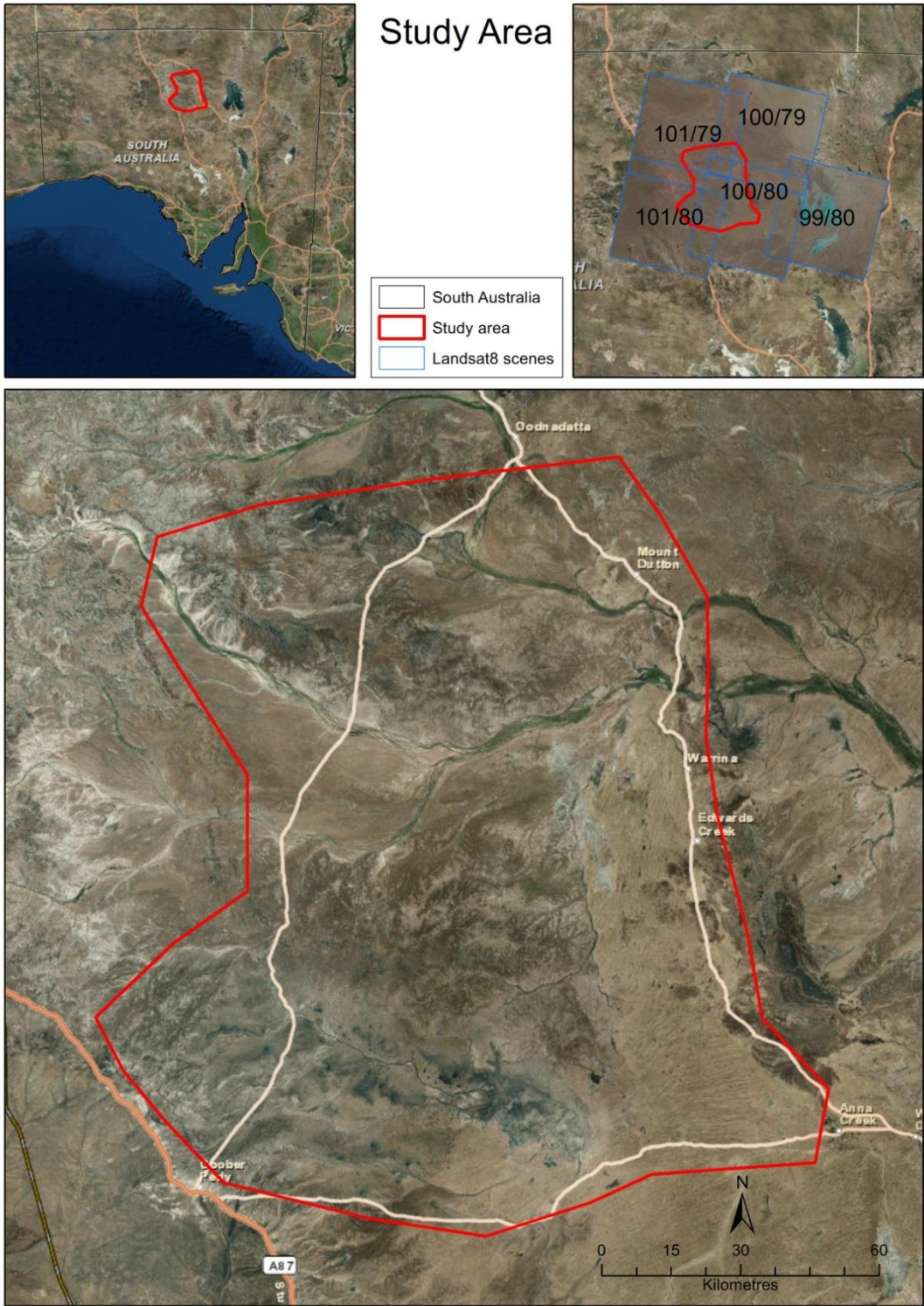


Figure 1: Study area

**Table 1: Landsat 8 Operational Land Imager (OLI) and Thermal Infrared Sensor (TIRS)**

\* TIRS bands are acquired at 100 metre resolution, but are resampled to 30 metres in the delivered data product

Bands	Wavelength (micrometres)	Resolution (metres)
Band 1 - Coastal aerosol	0.43 - 0.45	30
Band 2 - Blue	0.45 - 0.51	30
Band 3 - Green	0.53 - 0.59	30
Band 4 - Red	0.64 - 0.67	30
Band 5 - Near Infrared (NIR)	0.85 - 0.88	30
Band 6 - SWIR 1	1.57 - 1.65	30
Band 7 - SWIR 2	2.11 - 2.29	30
Band 8 - Panchromatic	0.50 - 0.68	15
Band 9 - Cirrus	1.36 - 1.38	30
Band 10 - Thermal Infrared (TIRS) 1	10.60 - 11.19	100 * (30)
Band 11 - Thermal Infrared (TIRS) 2	11.50 - 12.51	100 * (30)

The four Landsat scenes required to cover the contiguous study area are paths 100 and 101, rows 79 and 80 (Figure 1). These scenes include Freeling South and Francis Swamp. The Hermit Hill complex is covered by Path 99 Row 80.

Table 2 is a list of all Landsat images for path 100 and 101, available from the USGS, showing the acquisition date and percentage of cloud cover. Images in path 101 are acquired a week after images in path 100. A number of dates do not have images in the USGS library. Data highlighted in red in Table 2 are for those images with 0% cloud in the entire image for all four scenes. Those highlighted in blue are images with 0% cloud over the study area (but with cloud elsewhere in the scene) for all four scenes.

Ideally, we required a set of cloud-free images a month or two following rain, to allow for a green flush of vegetation, and a second set of images at the end of a dry spell. The dates of the images highlighted in either red or blue in Table 2 were compared to the rainfall data from Coober Pedy Airport (Table 3 and appendix 1).

Images from 2nd August 2014 (path 100) and 9th August 2014 (path 101) were downloaded as the best available to represent conditions following a wet period. They are the first set of clear images following the heavy rainfall in April. Images from 8th December 2014 (path 100) and 15th December 2014 (path 101) were used to represent dry conditions with negligible rain after May.

We also downloaded two cloud free images for scene 99, 80, covering the Hermit Hill Complex, for 27/07/2014 and 01/12/2014 (a week before the path 100 images).

**Table 2: Dates of Landsat 8 OLI TIRS L1T imagery (path/row) and % cloud cover**

All = entire image, AOI = area of interest i.e. study area

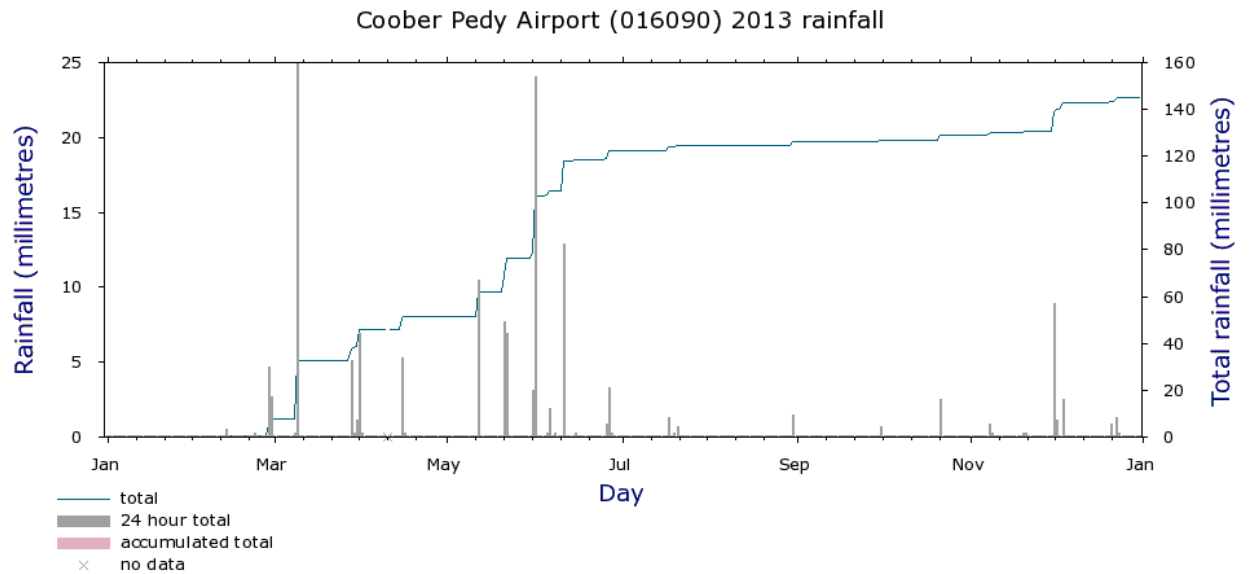
Red = 0% cloud in the entirety of the four images. Blue = 0% cloud in the study area within each of the four images, although some cloud elsewhere in the four images.

\* Downloaded 2<sup>nd</sup> August and 8<sup>th</sup> December 2014 for path 100; and 9<sup>th</sup> August 2014 and 15<sup>th</sup> December 2014 for path 101.

Path 100	% Cloud				Path 101	% Cloud			
	100/79		100/80			101/79		101/80	
	All	AOI	All	AOI		All	AOI	All	AOI
09/04/13	-	-	-	-	16/04/13	0	0	2	2
25/04/13	-	-	-	-	02/05/13	0	0	0	0
11/05/13	2	25	7	50	18/05/13	-	-	-	-
27/05/13	7	0	0	5	03/06/13	-	-	-	-
12/06/13	50	90	76	90	19/06/13	-	-	-	-
28/06/13	1	0	1	0	05/07/13	-	-	-	-
14/07/13	8	5	0	50	21/07/13	-	-	-	-
30/07/13	0	0	1	0	05/08/13	-	-	-	-
15/08/13	1	0	1	0	22/08/13	0	1	1	1
31/08/13	1	0	1	0	07/09/13	-	-	-	-
16/09/13	2	50	28	30	23/09/13	-	-	-	-
02/10/13	-	-	-	-	09/10/13	-	-	-	-
18/10/13	-	-	-	-	25/10/13	0	0	0	0
03/11/13	2	0	1	0	10/11/13	0	0	0	0
19/11/13	13	90	18	25	26/11/13	59	90	29	90
05/12/13	-	-	0	0	12/12/13	0	0	0	0
21/12/13	35	100	-	-	28/12/13	0	0	14	1
06/01/14	0	0	1	0	13/01/14	0	0	0	0
22/01/14	67	90	78	90	29/01/14	0	0	0	0
07/02/14	0	0	0	0	14/02/14	-	-	-	-
23/02/14	1	0	1	0	02/03/14	0	0	0	0
11/03/14	1	0	1	0	18/03/14	0	0	0	2
27/03/14	1	0	2	0	03/04/14	-	-	-	-
12/04/14	13	50	15	90	19/04/14	0	0	0	0
28/04/14	2	5	1	0	05/05/14	33	90	60	90
14/05/14	6	90	23	90	21/05/14	0	0	2	1
30/05/14	72	75	52	75	06/06/14	0	5	0	2
15/06/14	18	50	1	0	22/06/14	0	0	0	0
01/07/14	1	20	3	50	08/07/14	0	1	1	5
17/07/14	53	100	10	75	24/07/14	0	0	58	50
02/08/14	1	*0	1	*0	09/08/14	0	*0	0	*0
18/08/14	1	0	0	0	25/08/14	0	0	0	0
03/09/14	6	90	16	75	10/09/14	0	0	0	0
19/09/14	1	0	1	0	26/09/14	5	5	2	5
05/10/14	0	0	4	0	12/10/14	0	0	0	0
21/10/14	0	0	0	0	28/10/14	0	0	0	0
06/11/14	4	50	6	75	13/11/14	0	0	0	0
22/11/14	12	50	4	25	29/11/14	37	50	46	70
08/12/14	0	*0	0	*0	15/12/14	0	*0	0	*0
24/12/14	10	5	1	0	31/12/14	0	0	0	0
09/01/14	41	100	63	100	16/01/15	0	0	0	0

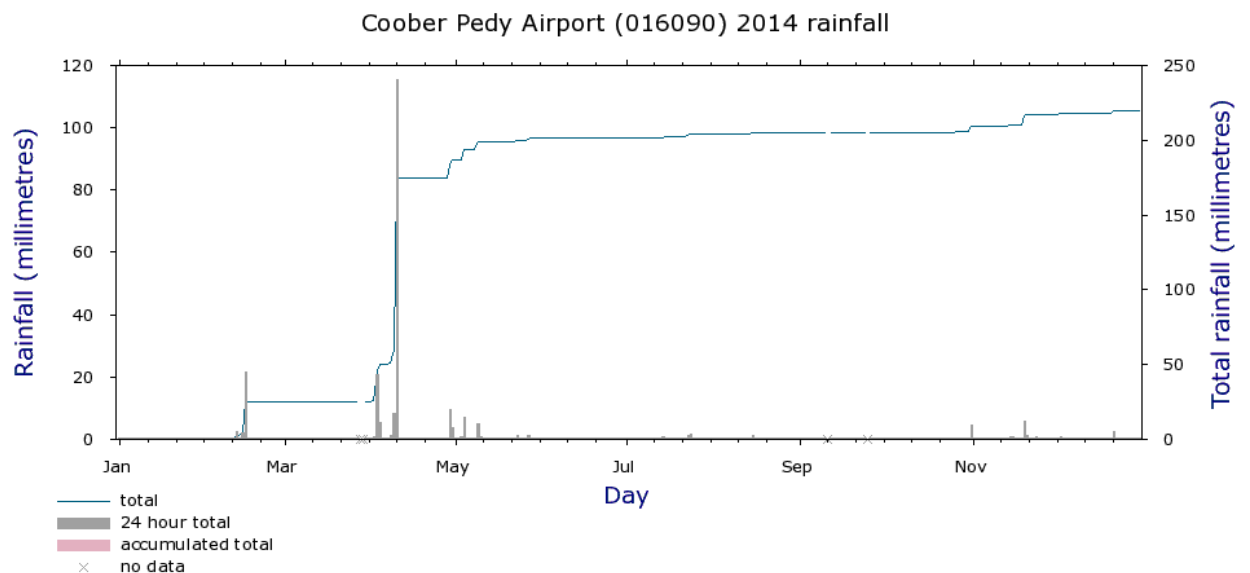
**Table 3: Coober Pedy airport monthly rainfall (mm)**

	Jan	Feb	Mar	Apr	May	Jun	Jul	Aug	Sep	Oct	Nov	Dec	Annual
2013	0.0	7.8	38.0	5.6	27.8	43.4	2.0	1.4	0.0	3.0	1.4	14.4	144.8
2014	0.0	25.0	0.0	161.6	14.6	0.2	3.0	0.8	0.2	0.2	11.6	2.6	219.8
Summary statistics for all years 1994 - 2014													
<b>Mean</b>	13.1	14.9	9.4	14.0	9.0	12.2	5.1	6.2	7.1	11.6	12.7	18.6	
<b>Median</b>	5.3	7.5	0.8	4.6	2.5	4.3	2.0	1.9	4.6	5.4	11.6	14.4	
<b>Highest Daily</b>	49.6	40.0	42.0	115.0	46.2	40.0	7.2	19.0	16.2	22.2	31.0	31.0	



Note: Data may not have completed quality control.

Climate Data Online, Bureau of Meteorology  
Copyright Commonwealth of Australia, 2015



Note: Data may not have completed quality control.

Climate Data Online, Bureau of Meteorology  
Copyright Commonwealth of Australia, 2015

Source: BOM 2015 <http://www.bom.gov.au/climate/data/index.shtml>



## 2.3 Satellite image pre-processing

Upon acquisition, georegistration of all USGS images was checked, and no further geographic correction was necessary. However, to ensure accurate and consistent measurements, radiometric calibration of all images is essential (USGS 2013).

Hence, a top-of-atmosphere reflectance correction was performed on all OLI bands (bands 1 to 7) of the images using the equations supplied by the United States Geological Survey (USGS, 2013). This removes the cosine effect of different solar zenith angles due to the solar time difference between data acquisition at different times of year. It also compensates for different values of the exoatmospheric solar irradiance arising from spectral band differences, and corrects for the variation in the earth-sun distance between different acquisition dates. These conversions provide a basis for standardised comparison of data between images acquired on different dates, or by different sensors.

Atmospheric correction to reflectance at land surface was not performed, because 1) no reliable dark pixel pseudo-invariant target was available in the study area, and 2) no direct atmospheric profile information was available. However, considering that our methods rely on albedo and emittance, atmospheric differences between dates are not anticipated to significantly influence either method. In the former case, atmospheric haze or absorption would be expected to influence reflectance in relatively small parts of the spectrum, and the measure of overall albedo across the whole spectrum would be little changed. In the latter case, emitted thermal radiation is very weakly interactive with atmospheric haze.

The OLI bands for the five images for August and the five images for December were mosaicked to form two images (each with the OLI bands 1-7), one for the wetter period (August) and one for the drier (December). Where there is an overlap in the images, the data was chosen from the various scenes using the following priorities, (path/row from highest to lowest priority):

- 100/80
- 100/79
- 101/80
- 101/79
- 99/80

An analysis mask was created to exclude Lake Eyre to the east and cloud in the south west from both mosaics (Figure 2a); as well as a thin band of cloud west of Lake Eyre in the summer mosaic (Figure 2b).

Only thermal band 10 was used in this analysis as a problem with band 11 calibration was reported in October 2014 (see <http://landsat.gsfc.nasa.gov/?p=9308> for details). A conversion to at-satellite brightness temperature (degrees Kelvin) was performed on the TIRS band 10 images (USGS 2013). The pixel values were converted to degrees centigrade by subtracting 273.15.

Because there can be a large difference in temperature regionally between different dates, the thermal images (TIRS band 10) were mosaicked by date (i.e. per Landsat path). This resulted in 3 thermal image strips for the wetter period (27th July for path 99, 2nd August for path 100 and 9th August for path 101) and 3 image strips for the drier period (1st December for path 99, 8th December 2014 for path 100 and 15th December for path 101). Finally, the analysis mask was applied to the temperature mosaics.

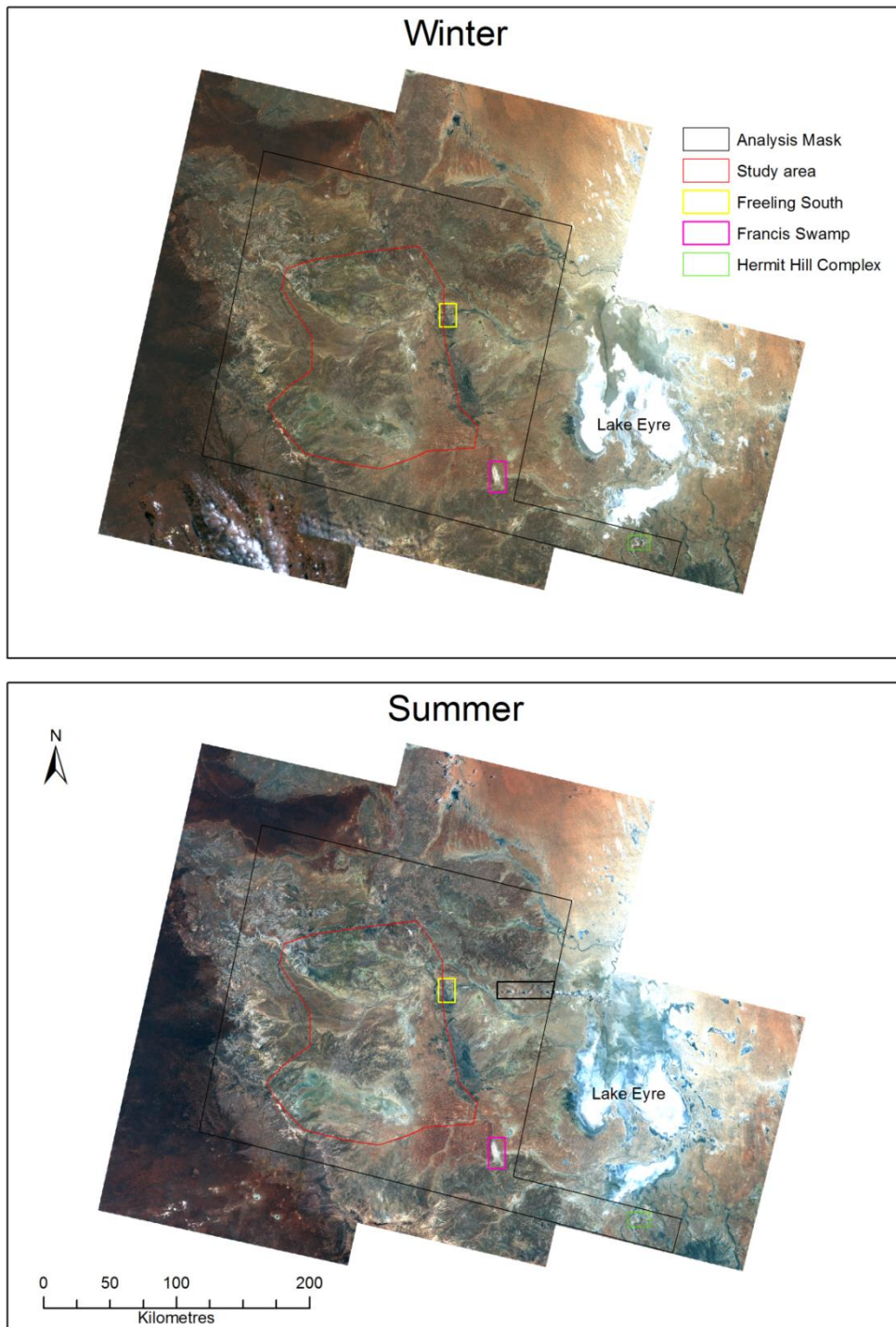


**Figure 2: Analysis mask covering the study area, Francis Swamp, Freeling South and the Hermit Hill Complex for both the (a) winter and (b) summer mosaicked Landsat imagery**

## 2.4 Training and evaluation data

The following methods require independent data on the location of some areas of diffuse discharge (evaporite minerals and wet soils), for both method training and evaluation of the accuracy of resultant maps. Unfortunately, this data is extremely limited. We used the only available spatial datasets of the extent of diffuse discharge, from within or close to the prescribed study area, as training and evaluation data. The majority of these data were a product of the Allocating Water and Maintaining Springs in the Great Artesian Basin (AWMSGAB) project (2008-2012), commissioned by the National Water Commission (Gotch 2013; White et. al. 2013).

### 2.4.1 Lewis data

Outside the prescribed study area, but within the same region, evaporite minerals (diffuse discharge) and/or wet soil area (Near Surface Moisture Index – NSMI) have been mapped by White et.al. (2013) at Freeling South, Francis Swamp, and the Hermit Hill Complex (Figure 2) as part of the AWMSGAB project. These areas had been chosen for the Lewis study because they are representative of the diversity of spring forms and vegetation communities present in this part of the Great Artesian Basin. Mapping for that project was from HyMap airborne hyperspectral imagery with 128 spectral bands at resolution of approximately 3 metres during 2009 and 2011, as well as 2001 archival ASTER thermal imagery at moderate resolution (90 metre) for Francis Swamp. Some of these data were supplied to this project as raster layers (henceforth referred to as the “Lewis” data) (Table 4, Figures 3-5).

**Table 4: The Lewis datasets**

Area	Date	Data layers	Resolution
Francis Swamp	08-08-2001	ASTER Thermal	90 m
Freeling South	2011	Diffuse Discharge	3.0 m
Hermit Hill Complex	2009	Diffuse Discharge	3.2 m
Hermit Hill Group (within the Hermit Hill Complex)	2011	Diffuse Discharge	3.1 m
West Finnis Group (within the Hermit Hill Complex)	2011	Diffuse Discharge	3.1 m
Francis Swamp	2009	Near Surface Moisture Index (NSMI)	3.1 m
Freeling	2011	Near Surface Moisture Index (NSMI)	3.0 m
Hermit Hill Complex	2009	Near Surface Moisture Index (NSMI)	3.2 m
Hermit Hill Complex	2011	Near Surface Moisture Index (NSMI)	3.1 m
Hermit Hill Complex	2009	NSMI Creek Mask	n/a

The Lewis data has been qualitatively evaluated in the field, but has not been subjected to a formal quantitative accuracy assessment. As such, it cannot be used to perform a quantitative validation of the diffuse discharge mapping methodology presented in this report. However, we can perform a qualitative evaluation of our methodology by comparing our results to the Lewis results.

The 2009 Hermit Hill Complex Lewis diffuse discharge data was used as training data for evaporite mineral detection. The Hermit Hill Complex 2009 NSMI data (Landsat path 099) was used as training data for setting a temperature threshold for wet area detection. The 2009 data was chosen in preference to the 2011 data for training purposes as the 2009 hyperspectral imagery was acquired in a drier period than the 2011 imagery. The other Lewis datasets were used in evaluating performance of the evaporite mineral detection and wet area mapping methods developed herein (Table 5).

#### **2.4.2 Gotch diffuse discharge data**

Within the prescribed study area itself, there was previously no independent mapping of diffuse discharge zones. Travis Gotch, an expert familiar with the area, digitised areas of ‘potential’ diffuse discharge within the study area for this project (henceforth referred to as the “Gotch diffuse discharge” data).

The eleven areas (polygons) of potential diffuse discharge identified are not intended to be exact representations of where evaporite minerals are thought to exist, but rather an approximate indication of general areas where Travis Gotch knows or suspects they will be found. Some of the polygons are likely to be almost entirely diffuse discharge, while others are expected to only contain small or fragmented areas within the defined polygon, and no diffuse discharge is expected to be found in inner polygon 9. As such, this data also cannot be used for a formal quantitative validation of the area mapped by our methodology. We can only evaluate if, and how much, diffuse discharge was detected in each polygon.

The Gotch diffuse discharge dataset was divided into five training and six evaluation polygons (Table 5, Figure 6a).

#### **2.4.3 Gotch spring vent data**

There is also a record of surveyed and un-surveyed spring vents, which includes sites inside and outside the study area, resulting from the AWMSGAB project (Gotch 2013; White et. al. 2013).

The inventory data for the surveyed records (GAB springs RTK) includes GPS coordinates and information on water flow (extinct, dry, damp, saturated, free water or free water and tail) for almost half the vents. Other inventory attributes include elevation, pH, substrate, flora and fauna. RTK (Real Time Kinematic) surveying improves the accuracy of GPS positions, and these records of spring vents are considered the most precise in the SA portion of the GAB (Gotch 2013).

Due to record rainfall events across much of the region during the AWMSGAB project, a number of spring groups remained un-surveyed. The data for these records was sourced from previous work (e.g. Niejalke, 1996 via Gotch 2013). The GPS data for the un-surveyed records (GAB springs non-RTK) was collected while Selective Availability of the GPS signal was on, reducing the accuracy of these positions.

Travis Gotch also supplied a point shapefile of the ‘estimation’ of locations of five spring vents in the Toodina area.

These three datasets are henceforth referred to as the “Gotch springs” data (Table 5, Figure 6b). They were clipped to the analysis mask resulting in 2,866 RTK, 63 non-RTK and 5 Toodina records.

Throughout the western Great Artesian Basin much diffuse discharge is associated with spring vents. However, diffuse discharge may occur in areas without vents and vents are not always accompanied by diffuse discharge. Thus the vent data cannot be used for training purposes. It can only be used as an indication of whether our methodology is mapping diffuse discharge in areas it is likely to be found.

**Table 5: Training and evaluation datasets**

Name	Year	Data type	Albedo (evaporite)	Temperature (wet area)	Albedo + Temp (current discharge)
<b>Training Data</b>					
Hermit Hill Complex	2009	Diffuse Discharge	X	-	
Hermit Hill Complex	2009	NSMI	-	X	
Gotch polygon 2	2015	Sketch	X	X	
Gotch polygon 4	2015	Sketch	X	X	
Gotch polygon 6	2015	Sketch	X	X	
Gotch polygon 8	2015	Sketch	X	X	
Gotch polygon 11	2015	Sketch	X	X	
<b>Evaluation Data</b>					
Freeling South	2011	Diffuse Discharge	X	-	
Hermit Hill Group	2011	Diffuse Discharge	X	-	
West Finnis Group	2011	Diffuse Discharge	X	-	
Freeling	2011	NSMI	-	X	
Francis Swamp	2001	Thermal	-	X	
Francis Swamp	2009	NSMI	-	X	
Hermit Hill Complex	2011	NSMI	-	X	
Gotch polygon 1	2015	Sketch	X	X	X
Gotch polygon 3	2015	Sketch	X	X	X
Gotch polygon 5	2015	Sketch	X	X	X
Gotch polygon 7	2015	Sketch	X	X	X
Gotch polygon 9	2015	Sketch	X	X	X
Gotch polygon 10	2015	Sketch	X	X	X
Gotch Springs - RTK	Post 2000	Point Shapefile	X	X	X
Gotch Springs - Non RTK	Pre 2000	Point Shapefile	X	X	X
Gotch Springs - Toodina estimates	2015	Point Shapefile	X	X	X

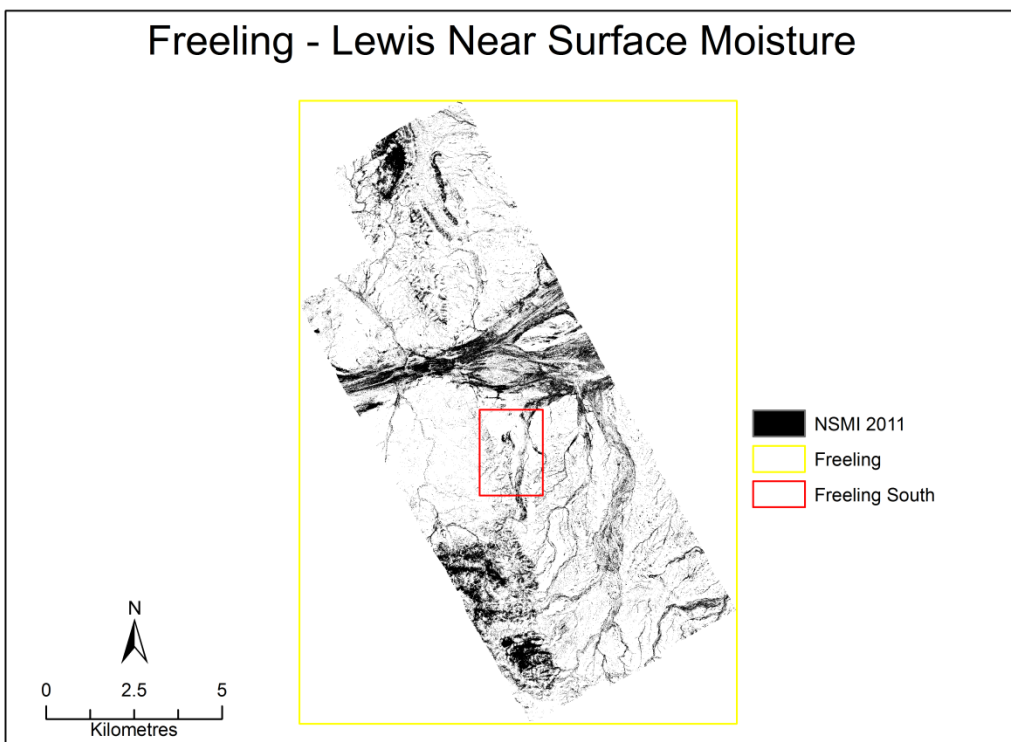
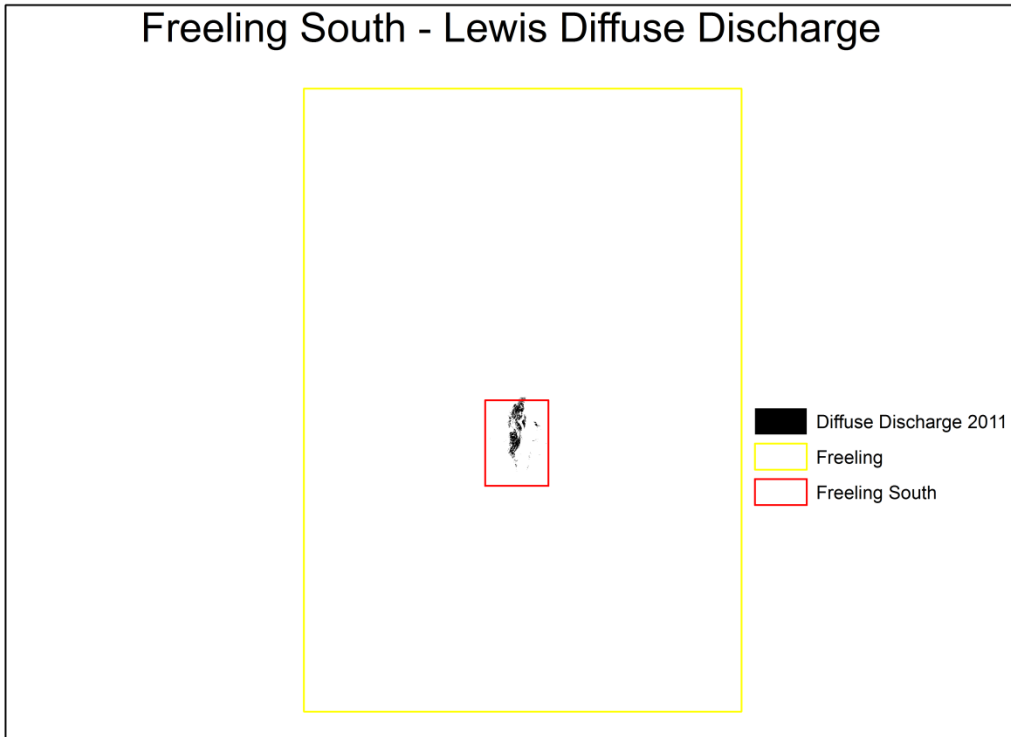


**Figure 3: Freeling South Lewis data (a) diffuse discharge 2011 (b) near surface moisture 2011**

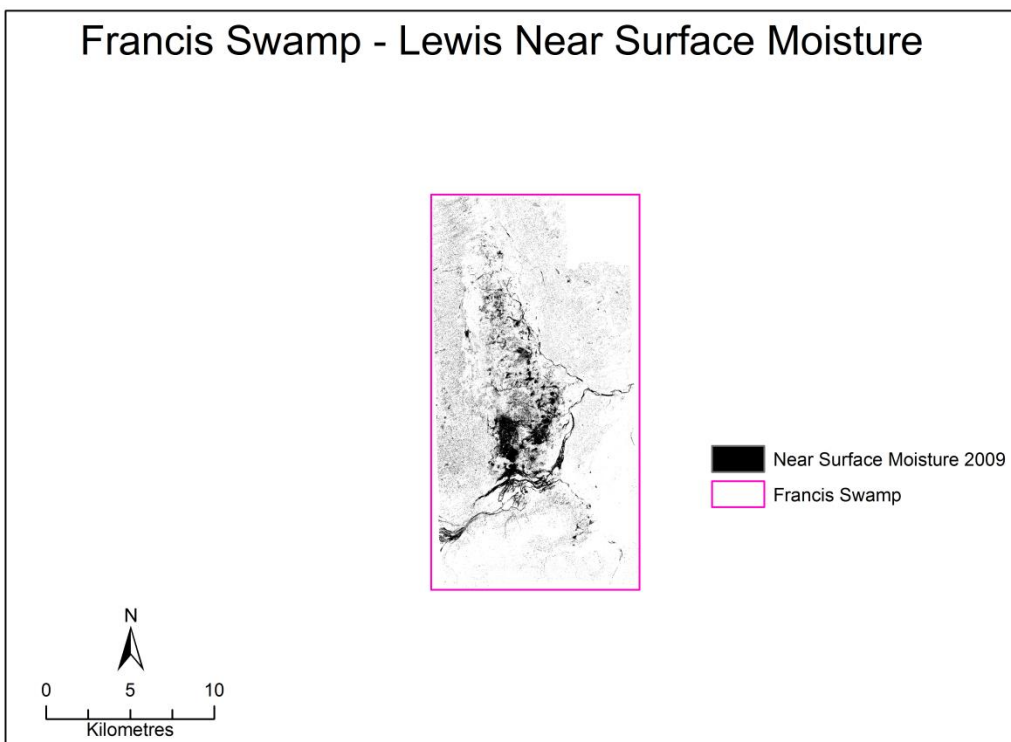
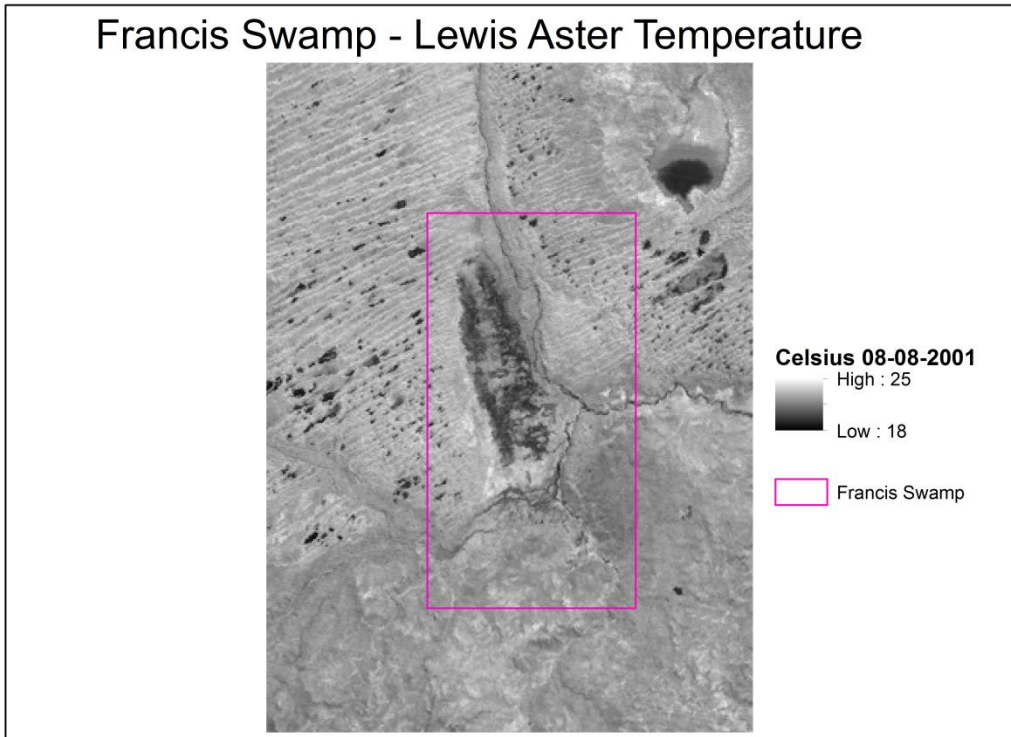
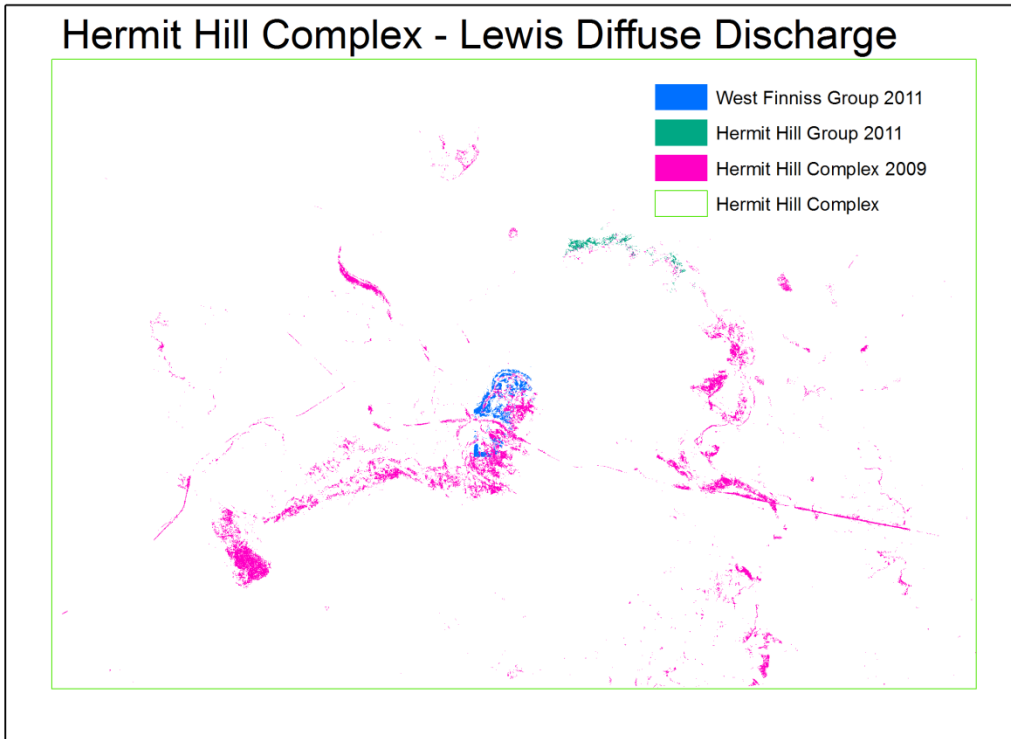


**Figure 4: Francis Swamp Lewis data (a) ASTER temperature 2001 (b) near surface moisture 2009**



### Hermit Hill Complex - Lewis Near Surface Moisture

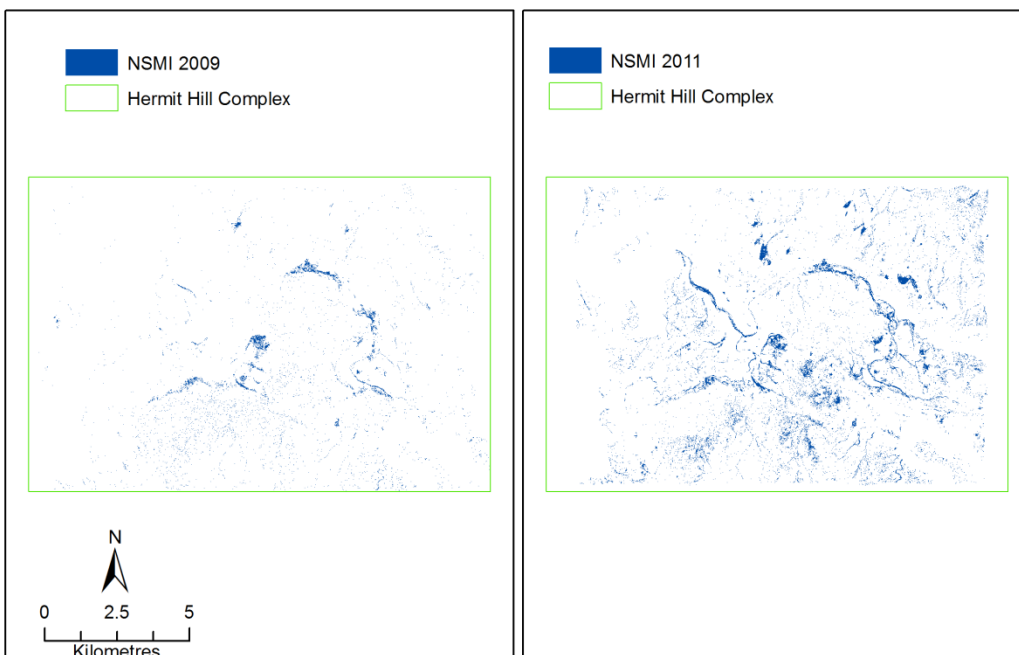


**Figure 5: Hermit Hill Complex Lewis data (a) diffuse discharge 2009 and 2011 (b) near surface moisture 2009 (c) near surface moisture 2011**



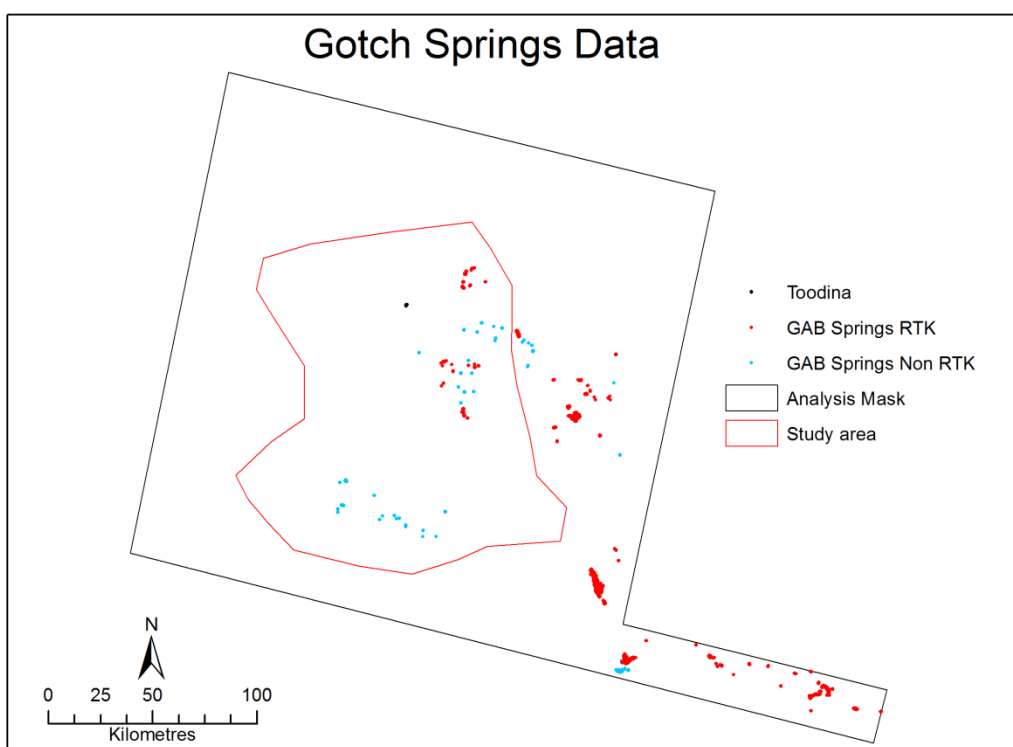
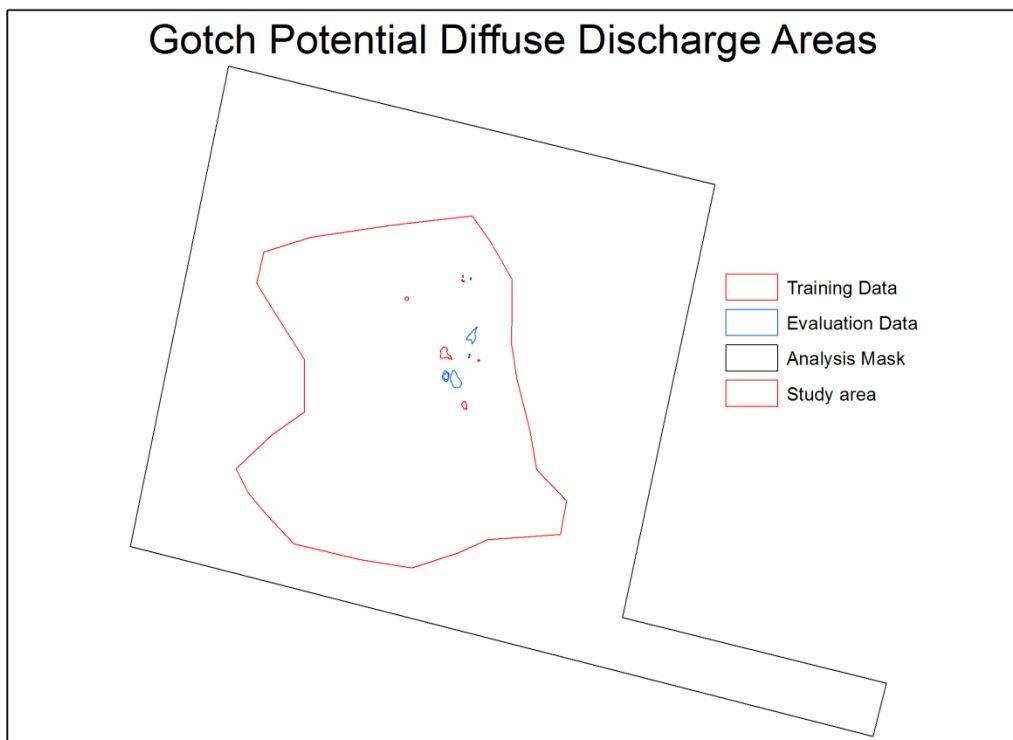


**Figure 6: (a) Gotch potential diffuse discharge areas divided into training and evaluation data (b) Gotch springs data**

## **2.5 Evaporite mineral detection – Historical and current discharge**

Evaporite mineral deposits reflect strongly across all of the electromagnetic spectrum covered by the OLI instrument, unlike most other land covers in the region. However, some bright sands and soils have somewhat similar reflectance profiles.

We used a measure of overall brightness in all OLI bands as an approximation of land surface albedo (total reflectance over visible – infrared wavelengths) to map areas of evaporite minerals. This was done using Principal Components Analysis, which can be easily automated.

Principal Components Analysis (PCA) is a linear transformation technique related to Factor Analysis. Given a set of correlated image bands, PCA produces a new set of images, known as components, which are uncorrelated with one another and are ordered in terms of the amount of variance they explain from the original data set. For a typical multispectral image band set, it is common to find that the first two or three components are able to explain a very high proportion of the original variability in reflectance values. Later components tend to be dominated by smaller scene components and instrument noise effects.

We performed a PCA on the OLI bands (Bands 1-7) of:

- the winter mosaic (7 principal components)
- the summer mosaic (7 principal components)
- the winter and summer mosaics in combination (14 principal components)

The first principal component (PC1) of each PCA was a weighted sum of the OLI bands and produced an image highlighting areas that were bright in:

- winter
- summer
- both winter and summer

The values of PC1 were compared with the Lewis Hermit Hill 2009 diffuse discharge data in particular, but also with the Gotch training areas of potential diffuse discharge. A threshold of albedo (i.e. the higher values of PC1) was set. Above this brightness areas are more likely to be evaporite minerals, while areas below the threshold are more likely to be bare soil, vegetation or water.

## **2.6 Wet ground detection – Current discharge**

Active diffuse discharge results in areas of damp soils. As water evaporates the state-change from liquid to gas absorbs significant amounts of energy from the environment, and results in soil cooler than the ambient temperature. Hence, mapping of lower temperature areas from remotely sensed thermal imagery can theoretically detect areas of damp soil. Use of thermal satellite imagery for mapping

current diffuse discharge areas associated with GAB springs is illustrated in White et. al. (2013).

We used the brightness temperature recorded by the TIRS sensor to map these areas of cooler, and therefore probably wet, soils in each of the Landsat thermal strips for band 10:

- path 99 winter
- path 100 winter
- path 101 winter
- path 99 summer
- path 100 summer
- path 101 summer

Because there can be a large difference in temperature regionally between different dates, a separate threshold was calculated for each of these thermal strips. This was done using the 2009 Hermit Hill Complex Near Surface Moisture Index (NSMI) for path 99, and the Gotch training polygons for path 100, as training data. The threshold for path 101 was extrapolated from these.

We applied these thresholds to each of the six thermal strips (three summer and three winter). We also intersected the results of the winter and summer thresholds to obtain areas that were cool in both winter and summer.

Areas below these thresholds of brightness temperature are indicative of active diffuse discharge evaporation, of standing water (e.g., stream flow, pond or lake, or artificial water storage), or other near surface groundwater.

## **2.7 Combined evaporite mineral and wet ground detection**

We attempted to eliminate areas of standing water by masking with the mapped evaporite minerals extent; retaining only those wet areas coincident with a bright evaporite crust.

The raster PC1 albedo threshold layers for winter and summer were each converted to polygons. Each of the three temperature thresholds (path 099, 100 and 101) were converted to polygons and merged into one temperature threshold file for winter and summer. Each of the albedo threshold polygons was then intersected with the temperature polygon layer to give final combinations.

## **2.8 Accuracy evaluations**

We applied the evaporite mineral and wet ground detection methods and the intersection of both within the analysis mask, which includes the prescribed study area and also Freeling South, Francis Swamp and the Hermit Hill Complex.

However, there is insufficient field-verified data in which we have confidence to perform a formal quantitative accuracy assessment of our methodology for mapping the extent of diffuse discharge (see section 2.4). Rather, we performed four qualitative accuracy evaluations of our mapping (Table 5):

- the mapped evaporite minerals areas were compared to the evaporite minerals areas mapped by Lewis (i.e. diffuse discharge at Freeling South in 2011 and the two groups within the Hermit Hill Complex in 2011), plus the Gotch evaluation polygons;
- the mapped cool (wet) areas were compared to the areas of wet ground mapped by Lewis (i.e. NSMI in Freeling 2011, Francis Swamp 2009 and the Hermit Hill Complex 2011, as well as the ASTER thermal data for Francis Swamp in 2001), plus the Gotch evaluation polygons;
- the combined mapped evaporite minerals and wet ground areas were compared to the diffuse discharge regions mapped by the Gotch evaluation data; and
- the mapped evaporite minerals areas, wet ground areas and the combined areas were compared to the surveyed (which includes an attribute on flow) and un-surveyed Gotch spring vents

## 3 Results

This section presents the results of our evaporite mineral, wet area and combined evaporite/wet area detections, and then presents the evaluations of these products against the evaluation datasets.

### 3.1 Evaporite mineral detection – Historical and current discharge

We present the results of our detection and analysis of areas that are particularly bright (have a high albedo) over winter or summer. This is an indication of the presence of evaporate minerals, which in turn is indicative of either current or historical diffuse discharge.

Figure 7 shows both the winter and summer Landsat true colour images for the Hermit Hill Complex and the Gotch areas of potential diffuse discharge. These images show the evaporite mineral deposits more clearly in the winter image in both areas. This is because the flush of green vegetation is lowering reflectance in the majority of the winter image, whereas in the summer image the bright soils are exposed.

The first component (PC1) of the Principal Component Analysis (PCA) for the winter OLI bands, the summer OLI bands, and both winter and summer OLI bands combined, are shown in Figure 8. These PC1 image products highlight areas that are bright across winter, summer or both for the entire analysis area (Figure 8a). The close-ups of the Hermit Hill complex (Figure 8b), and a subset of the Gotch areas of potential diffuse discharge (Figure 8c), highlight the fact that diffuse discharge is more distinguishable from the background area in the winter images. There is little contrast between the diffuse discharge and surrounding values in the summer (and hence combined winter and summer) images.

Zonal statistics were calculated for the Hermit Hill Complex diffuse discharge data from 2009 and also the training subset of the Gotch potential diffuse discharge areas on the values of the first principal component (PC1) of the winter and summer images (Table 6). Examination of the mean, standard deviation and range of values in the images confirms that the winter image differentiates the brighter areas better than the summer image (Table 6).

Consequently, further reporting of the analysis of evaporite mineral detection will be on the winter imagery only.

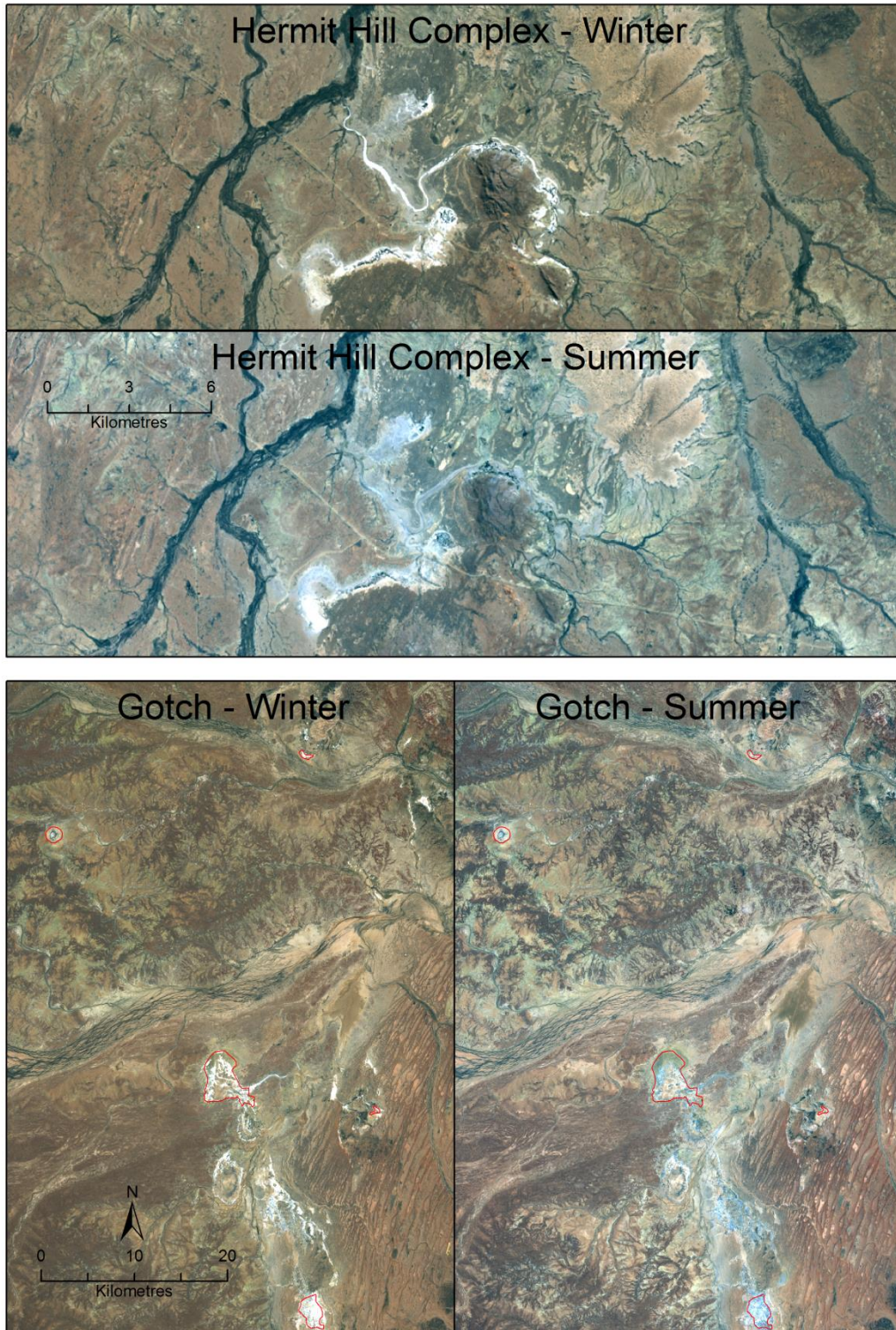


Figure 7: Winter and summer Landsat true colour images (red: band 4; green: band3; blue: band 2) for the Hermit Hill Complex and the Gotch potential diffuse discharge training areas

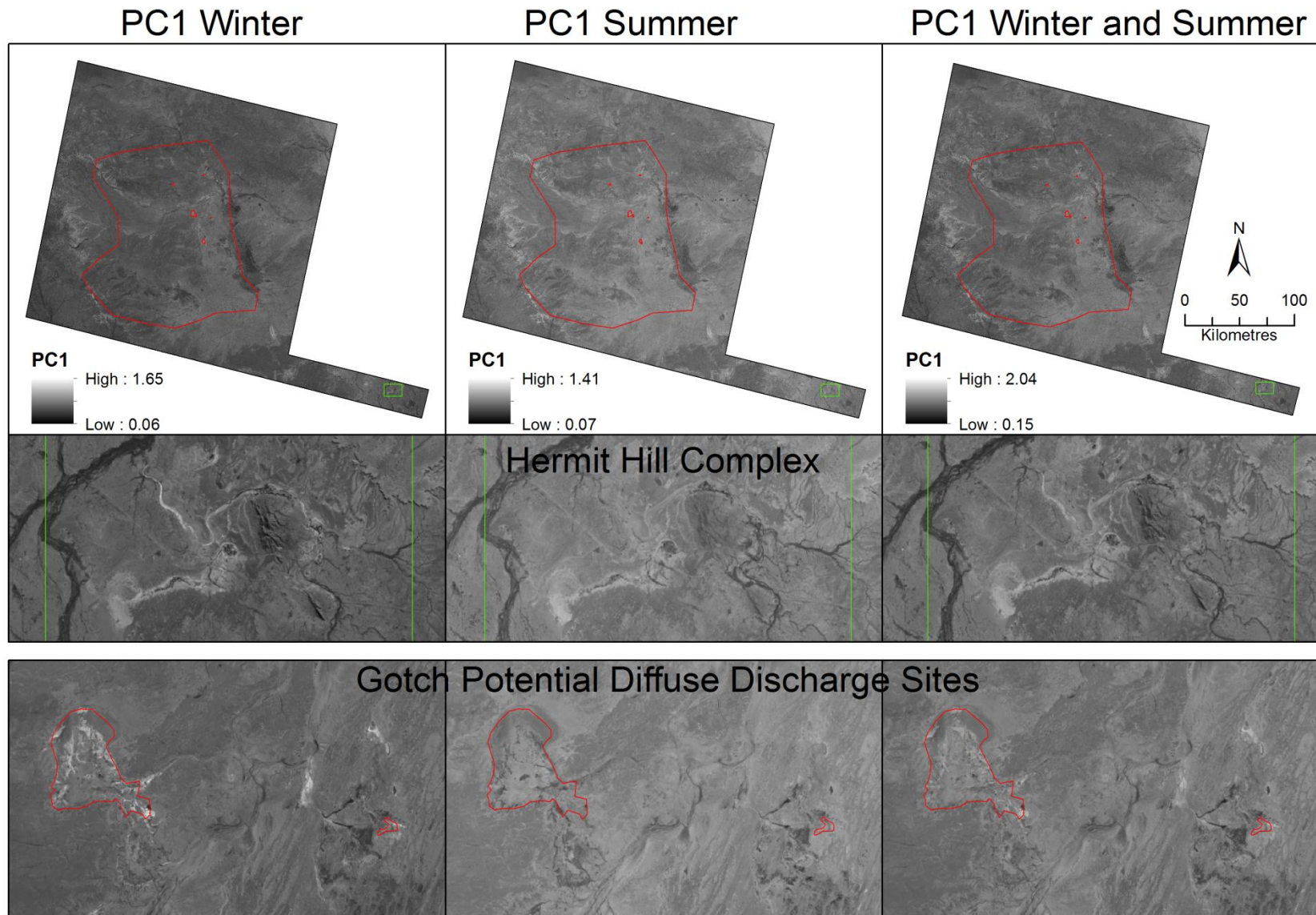


Figure 8: Principal Component 1 of combined OLI bands summer, winter and combined summer and winter mosaics (a) entire analysis area (b) Hermit Hill Complex (c) subset of training Gotch potential diffuse discharge areas

**Table 6: Zonal statistics of winter and summer Principal Component 1 (PC1) for the Lewis and Gotch diffuse discharge training datasets**

Area	Hectares	Min PC1	Mean PC1	Max PC1	STD PC1
<b>Winter PC1</b>					
Hermit Hill Complex DD 2009	234	0.39	0.80	1.24	0.14
Gotch DD Training Data 2014	2,771	0.20	0.80	1.57	0.13
All PC1 values 2014		0.06	0.61	1.65	0.09
<b>Summer PC1</b>					
Hermit Hill Complex DD 2009	234	0.40	0.77	1.07	0.16
Gotch DD Training Data 2014	2,771	0.37	0.75	1.02	0.10
All PC1 values 2014		0.07	0.70	1.41	0.09

The 2009 Lewis diffuse discharge data somewhat overmaps areas of diffuse discharge and misclassifies parts of the bright dirt on the Borefield Road and the Oodnadatta track as diffuse discharge (Figure 5a and Figure 10a). The Lewis diffuse discharge area also occupies a small amount of the darker areas in PC1 (as low as 0.39) (Table 6).

When determining a threshold for the winter PC1 that delineates diffuse discharge, the mean PC1 value for the Lewis Hermit Hill Complex diffuse discharge data and the Gotch training polygons was used as a starting point. Setting the threshold to 0.80 gave good coverage of the Lewis data (Figure 10b). Over 52% of the Lewis mapped diffuse discharge was co-incident with this threshold and it excluded the Lewis misclassified roads. However, this threshold resulted in over-mapping, and included areas which were not much brighter than their surroundings in the Landsat winter imagery (Figure 7a and Figure 10b).

To reduce this over-mapping, a higher PC1 threshold level was determined by increasing the threshold value by increments of 0.01 until a 'best fit' was obtained (minimizing over-mapping of darker areas, while retaining as much of the Lewis diffuse discharge area as possible). With a threshold value of 0.85 our evaporite extent was coincident with 41% of the Lewis data extent. The general distribution of the mapped evaporite area was the same as for 0.80, but with a thinning out of pixels with the lower values (Figure 10c). There is still an area in the north and east included in the 0.85 threshold which may not be evaporite, as it appears more like exposed soil in the Landsat winter imagery (Figure 7a and Figure 10c).

The final threshold was set at 0.90 (Figure 10d). It matches well with the Lewis data (excluding the Lewis road misclassifications) and has few pixels outside the Lewis shape, but with possibly some under-classification by us in the southeast area of evaporite. Areas above the 0.90 winter PC1 threshold are more likely to be evaporite minerals, and areas below that threshold are likely to be bare soil, vegetation or water.

The results of comparing the winter PC1 with the 0.85 and 0.90 threshold values to the Gotch potential diffuse discharge training sites can be seen in Figure 11. Once again the 0.85 threshold provides reasonable coverage of the bright areas in the training polygons, but also appears to over-map some areas along Peake Creek, which due to their location within a riparian corridor may simply be exposed, bright



soils (see Figure 11a). Raising the threshold to 0.90 decreases the area of potential evaporite by a small amount, but does decrease the possible misclassification along Peake Creek.

Figure 12 shows the results of applying the 0.85 and 0.90 PC1 thresholds to the entire analysis area. Both still include some areas of bright soil, particularly in the northeast corner of the analysis mask on the edge of the Simpson Desert and the bright mullock heaps (the earth and rock heaps from opal mining) near Coober Pedy in the southwest along the A87 road (Figure 9), both outside the actual study area. There is also a scattering of values above the PC1 threshold following the Peake Creek through the centre of the study area for the 0.85 threshold.

The majority of these possibly misclassified pixels are eliminated if the threshold is raised to 0.95.



**Figure 9: Mullock heaps from opal mining along the A87 outside Coober Pedy which have a very high albedo and a lower temperature than the surrounding red soil landscape**

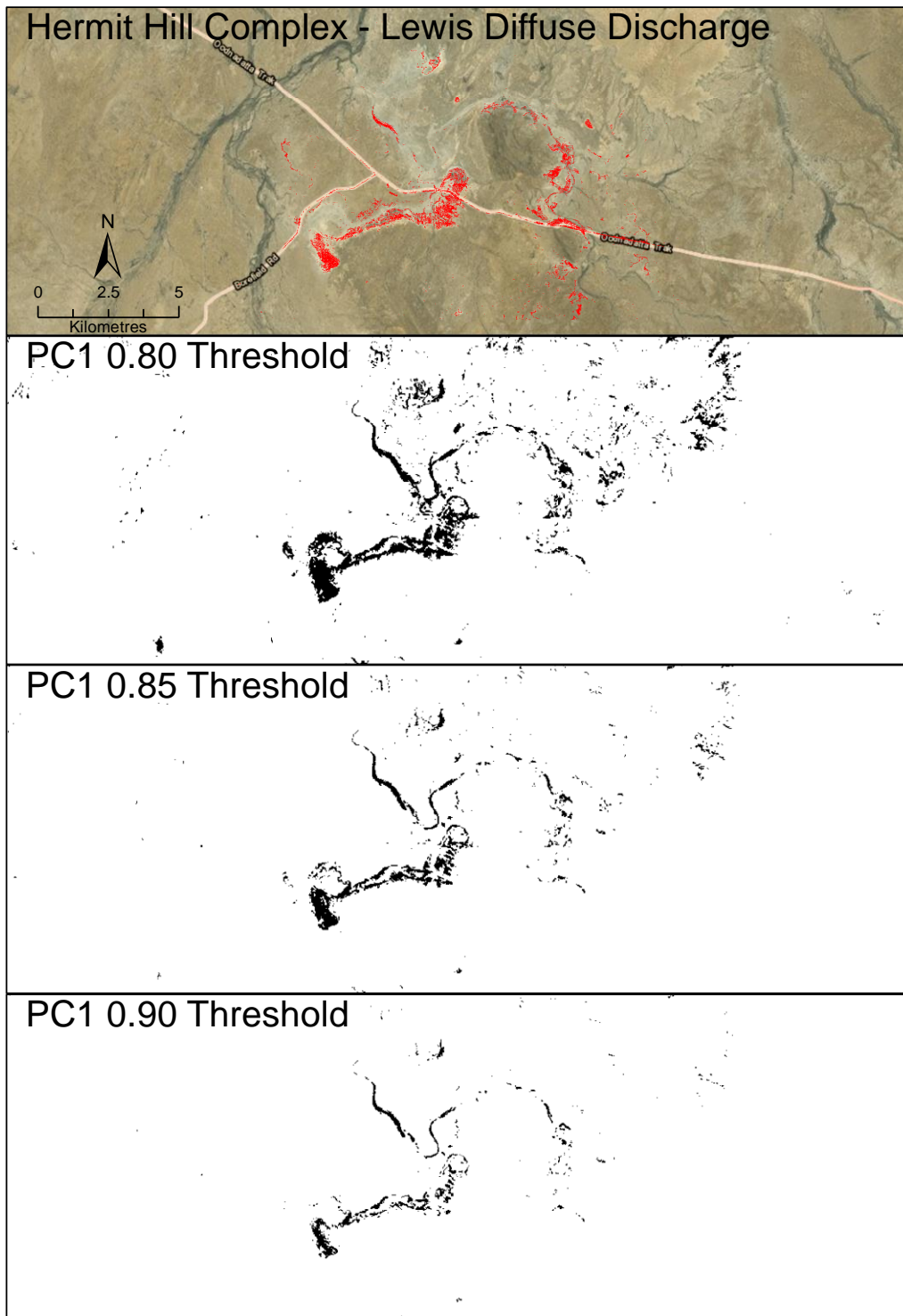


Figure 10: Hermit Hill winter Principal Component 1 thresholds for diffuse discharge (a) Hermit Hill Complex road network and Lewis diffuse discharge data (b) PC1 0.80 threshold (c) PC1 0.85 threshold (d) PC1 0.90 threshold

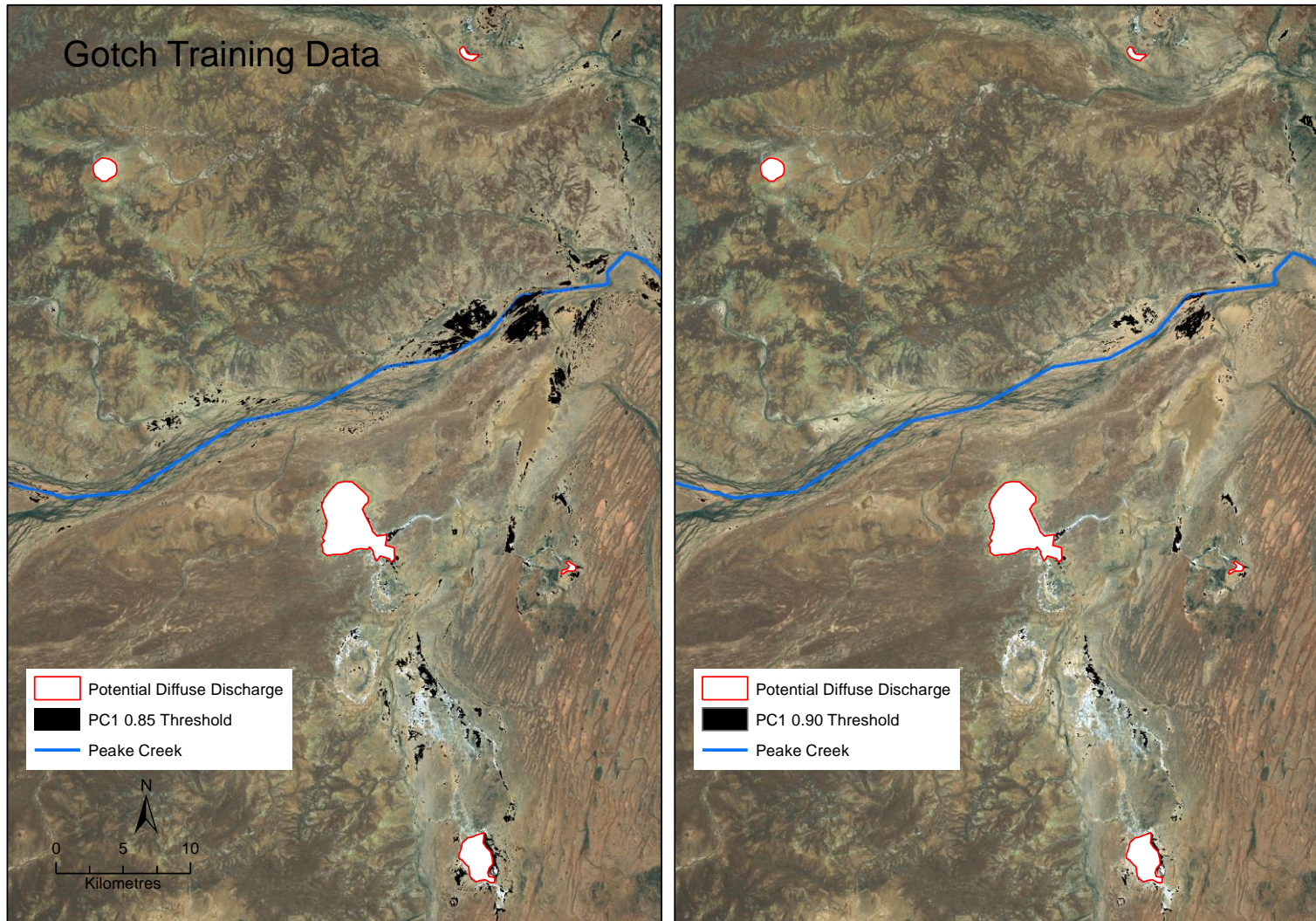


Figure 11: Principal Component 1 (PC1) diffuse discharge thresholds for the Gotch training areas (a) PC1 0.85 threshold (b) PC1 0.90 threshold

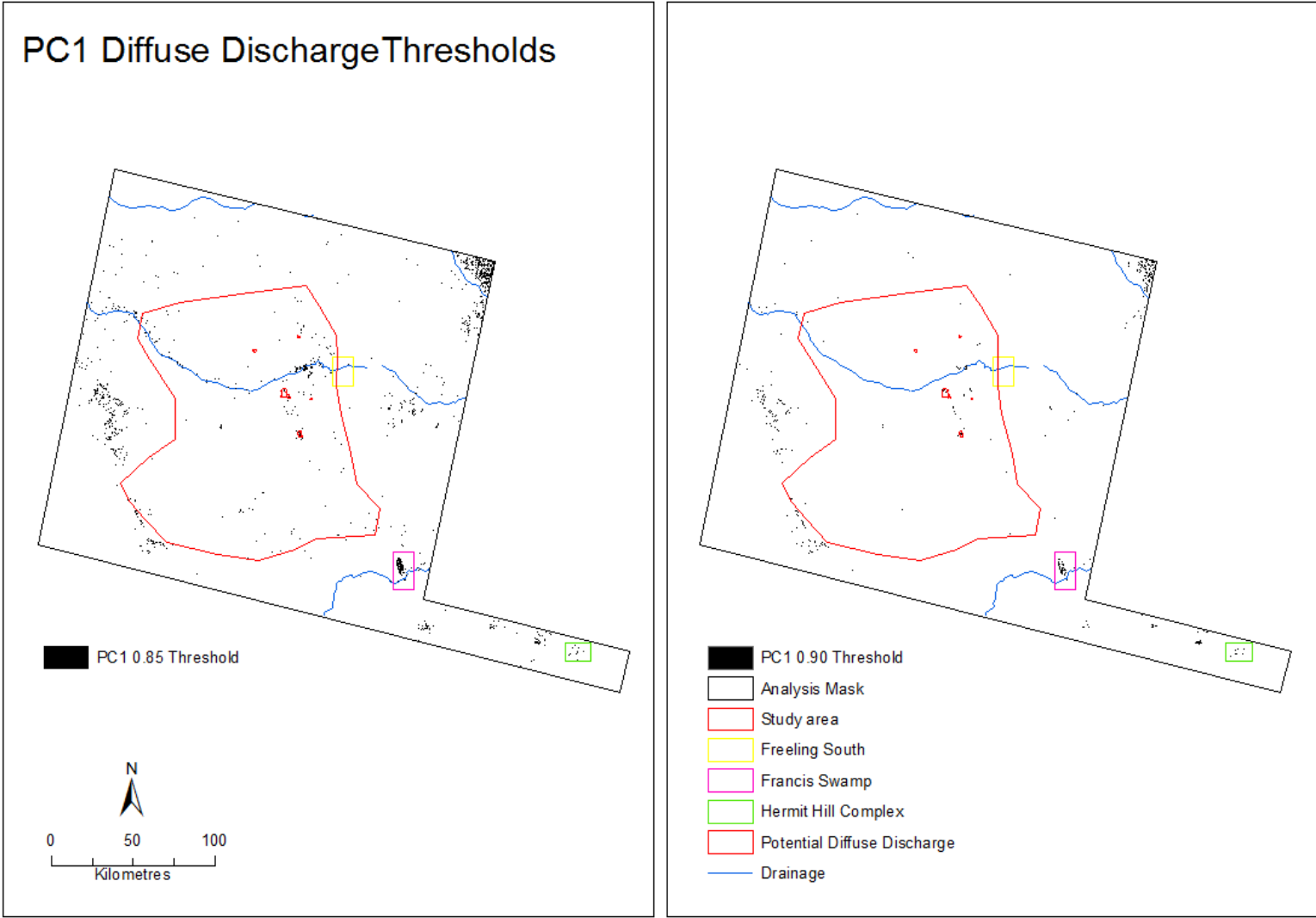


Figure 12: Principal Component 1 (PC1) diffuse discharge thresholds for the analysis area (a) PC1 0.85 threshold (b) PC1 0.90 threshold

### 3.2 Wet ground detection – Current discharge

We also present the results of our detection and analysis of areas that are colder than the surrounding area over winter and/or summer. This can be an indication of active diffuse discharge evaporation or of standing water.

The TIRS sensor band 10 temperature data was mosaicked by date/Landsat path, resulting in 3 winter and 3 summer thermal strips (Figure 13):

- path 99 winter
- path 100 winter
- path 101 winter
- path 99 summer
- path 100 summer
- path 101 summer

Zonal statistics were calculated for each thermal strip on the temperature pixel values (degrees Celsius). The difference in temperature between strips is evident from Table 7 and Figure 13.

Temperature zonal statistics were also calculated for the Hermit Hill 2009 NSMI pixels (Landsat path 090) and the Gotch training sites (path 100) as a training aid to setting a threshold temperature to map these areas of cooler, and therefore probably wet, soils. There was no training data for path 101.

The winter temperatures only were chosen for analysis as the temperature image for Landsat path 099 has large cool patches which appear to be damp from a rain shower. The east of the summer image for path 100 is also affected by a thin strip of cloud.

**Table 7: Statistics of band 10 temperature (degrees Celsius) for each Landsat 8 path for winter and summer images**

*Threshold = (mean temp – (STD \* 2)*

*\* The summer image for path 99 has large cool patches which look like it might be damp from rain*

*\*\* The east of the summer image for path 100 is masked for a strip of cloud cover*

Path / Date	Min temp °C	Mean temp °C	Max temp °C	STD temp °C
<b>Landsat Path 099</b>				
Path 99 Winter	9.63	18.29	23.44	1.13
Hermit Hill NSMI Winter	13.85	17.43	22.09	1.54
Path 99 Summer *	30.45	38.00	43.34	2.26
Hermit Hill NSMI Summer *	32.34	36.70	42.57	2.42
<b>Landsat Path 100</b>				
Path 100 Winter	4.19	15.21	20.97	0.81
Gotch training sites	6.54	14.29	18.01	1.87
Path 100 Summers **	28.05	43.45	50.67	1.49
Gotch training sites				
<b>Landsat Path 101</b>				
Path 101 Winter	8.00	23.08	29.90	1.73
Path101 Summer	35.18	45.46	55.31	2.57

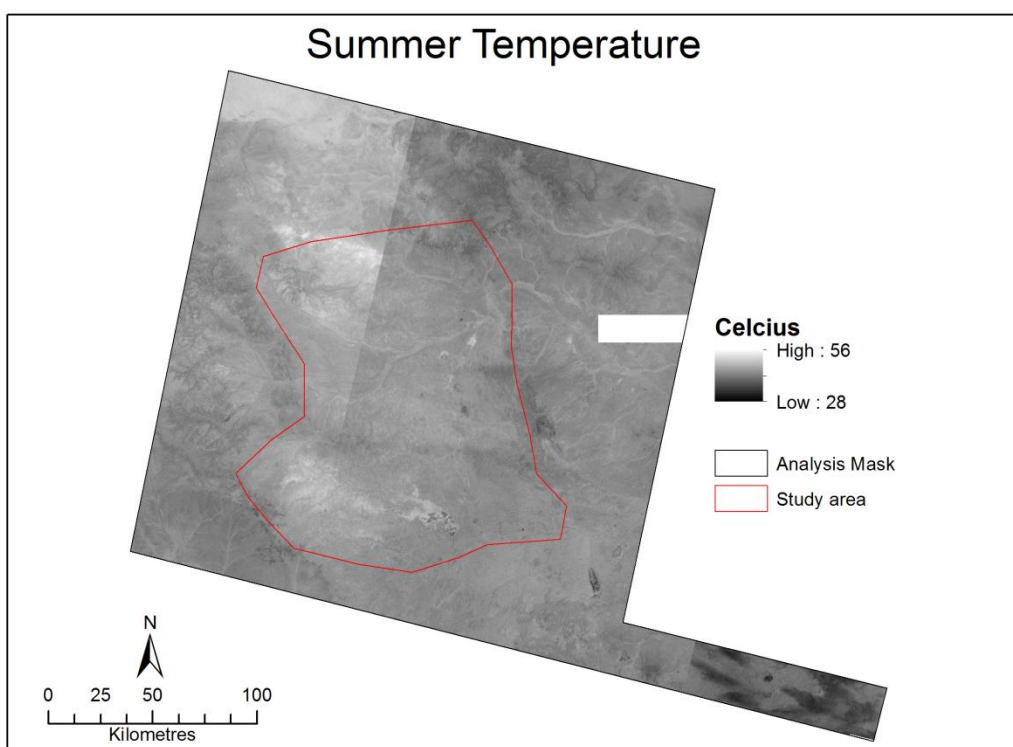
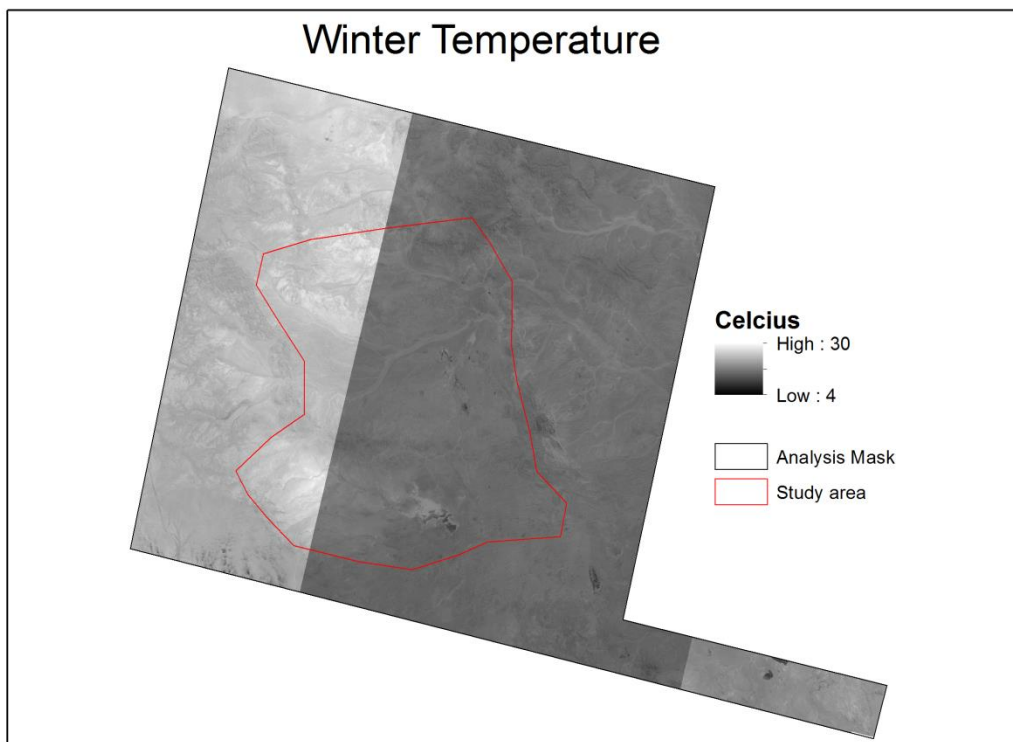


**Figure 13: Band 10 temperature (a) winter temperature mosaicked per Landsat path (b) summer temperature mosaicked per Landsat path**  
*Note the difference in background temperature between dates/Landsat paths*

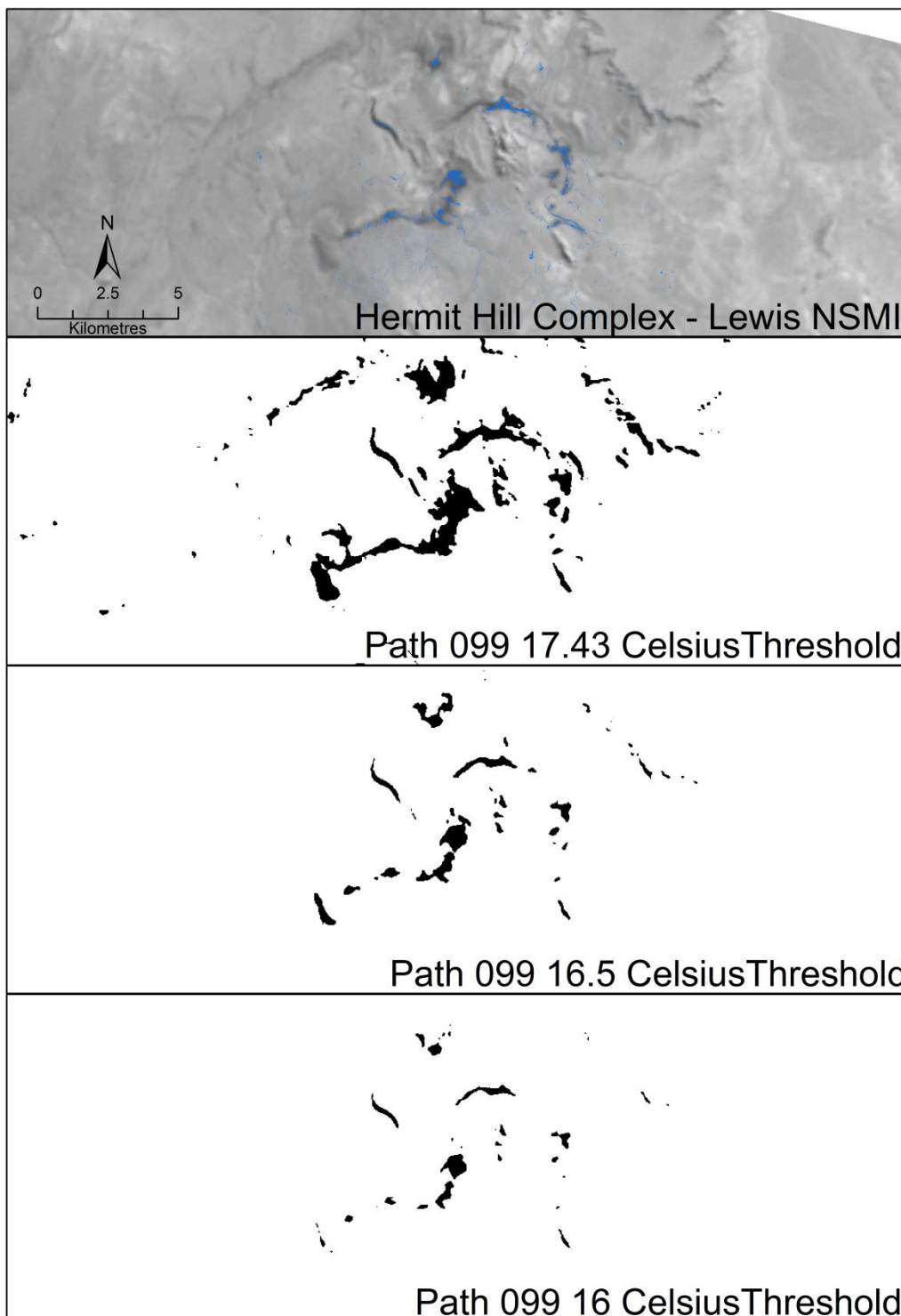


Figure 14: Hermit Hill winter temperature thresholds (Path 099) (a) Hermit Hill Complex and Lewis NSMI data (b) 17.43 °C threshold (c) 16.05 °C threshold (d) 16 °C threshold

The Hermit Hill Complex 2009 NSMI training data covers 176 hectares (Figure 14a). As with the principal components analysis, we used the mean of the training data as a starting point for determining a temperature threshold to detect potentially wet areas. For the Hermit Hill Complex this was 17.43 °C (Figure 14b). This is an overestimation, so decreases in 0.5 degrees were tested, starting at 17 °C.

The 16.5 °C threshold mapped 424 hectares, 56 ha of which overlap with the NSMI data (14c). The remaining NSMI data is predominantly very small areas scattered throughout the region. For a 16.0 °C threshold 216 hectares are mapped (14d). This is the best fit with the NRMI data and retains a 55 hectare overlap.

A similar methodology was followed on the Gotch training sites to arrive at a threshold of 13.5 °C (Figure 15).

The 16.0 °C threshold chosen for path 099 is approximately 2 standard deviations below the mean temperature ( $18.29 - (1.13 * 2) = 16.03$ ). This is also true of the threshold for path 100. As we do not have training data for path 101, this formula was used for estimating a threshold of 19.5 for path 101.

The combined thresholds (Landsat path 99, 100 and 101) are presented in Figure 16.

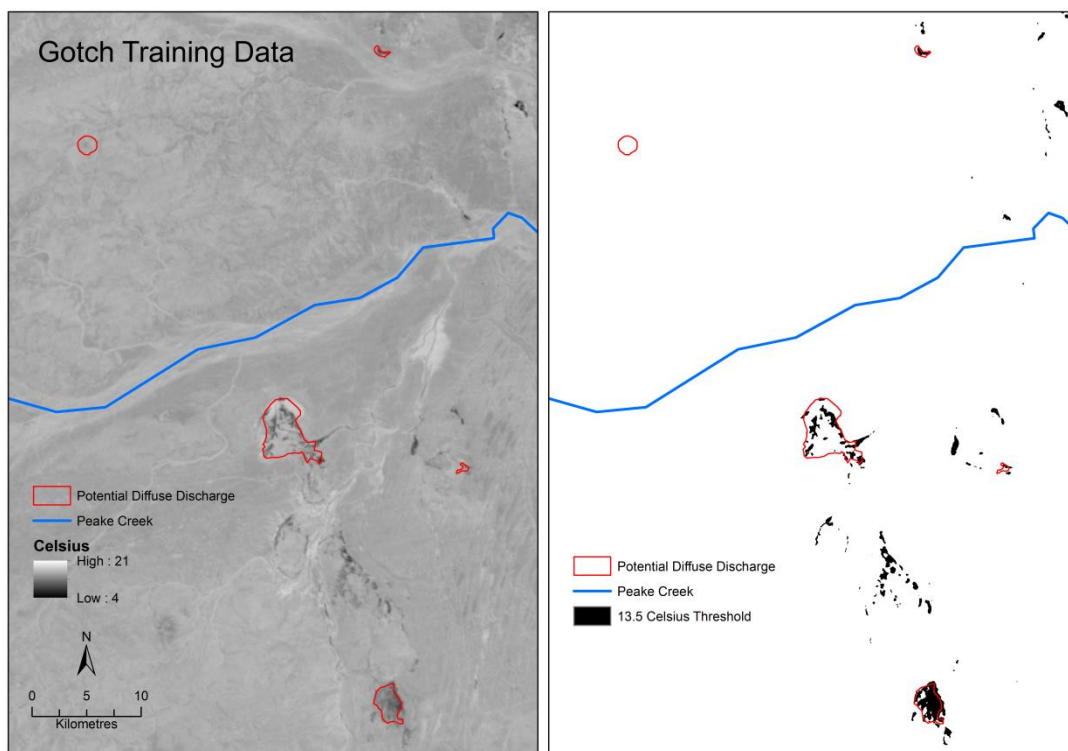


**Figure 15: Temperature threshold for the Gotch training areas (a) winter temperatures and training polygons (b) temperature threshold of 13.5 degrees Celsius**



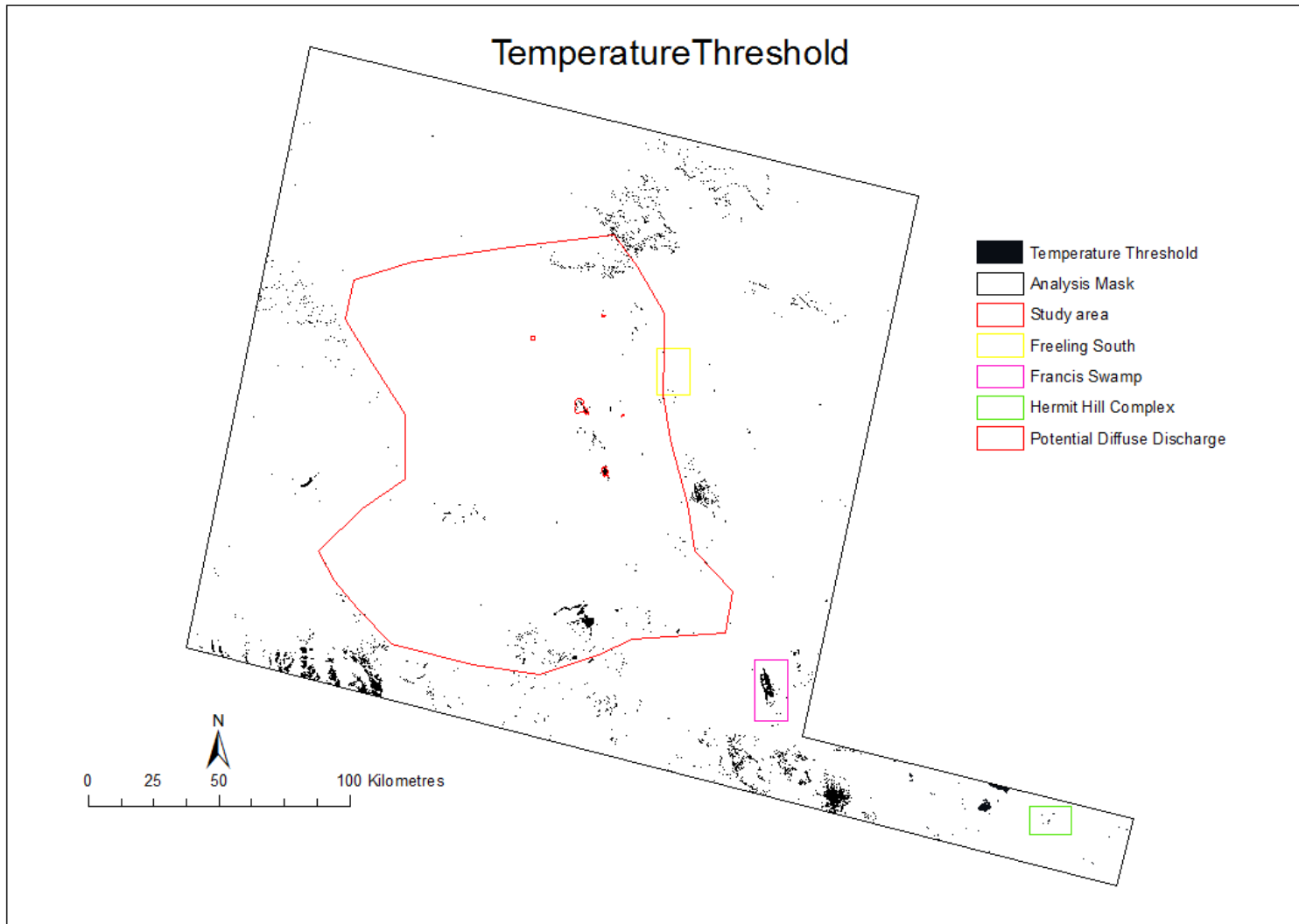
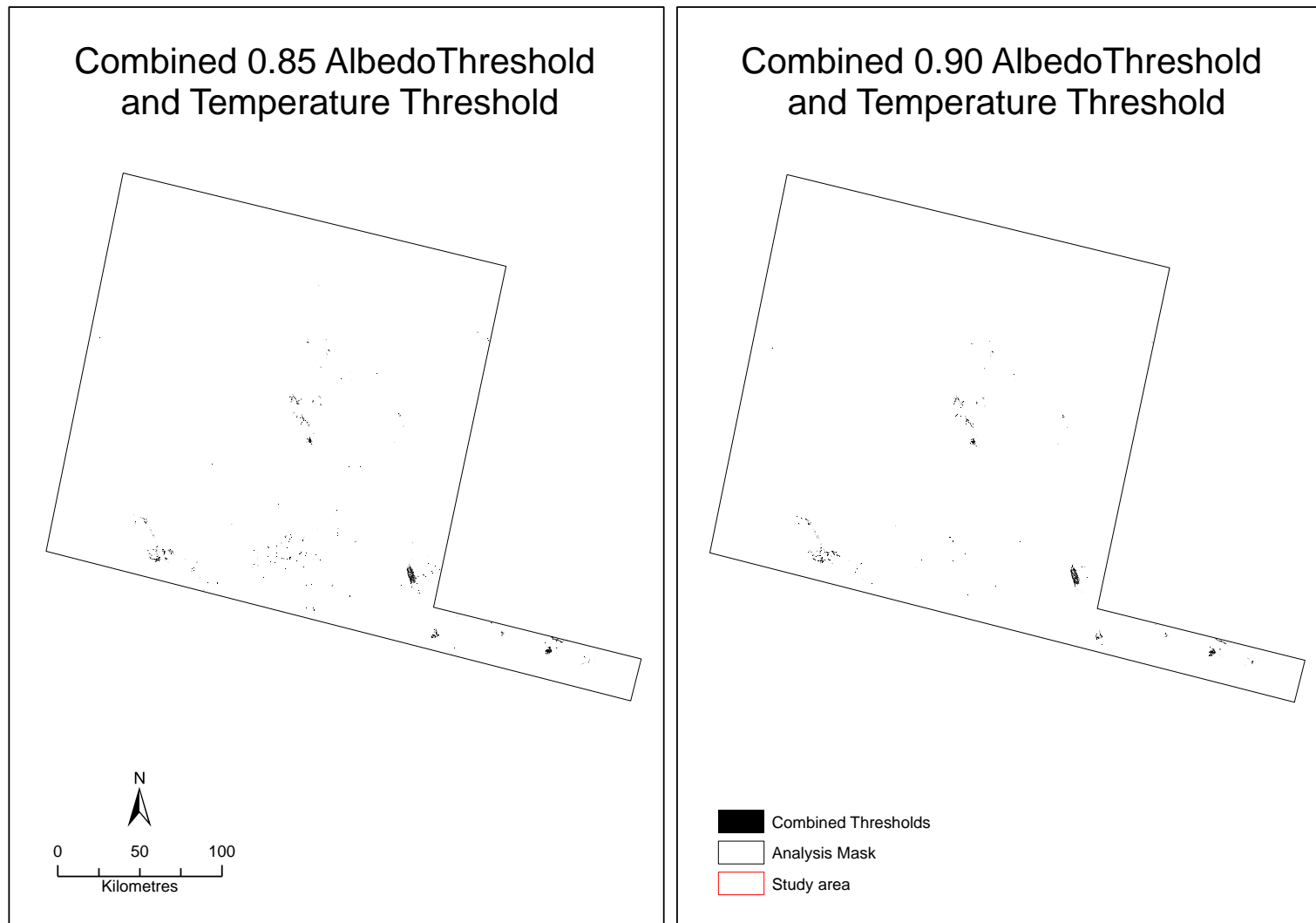


Figure 16: Temperature thresholds for the analysis area: Path 099 = 16 °C; Path 100 = 13.5 °C; Path 101 = 19.5 °C



**Figure 17: Combined PC1 albedo and temperature thresholds for the analysis area: (a) PC1 threshold of 0.85 + combined Landsat path temperature thresholds (b) PC1 threshold of 0.90 + combined Landsat path temperature thresholds**

*Note: due to the fine scale of this image not every point has been reproduced accurately. See enlargements in Appendix 2.*

### 3.3 Combined evaporite mineral and wet ground detection

We present the results of where areas of high albedo coincide with the cooler surface temperatures. This is very likely to be an indication that these bright areas contain water near the surface, i.e. current diffuse discharge. Standing water will have a darker albedo.

The results of combining each of the first principal component (PC1) albedo thresholds (0.85 and 0.90) with the temperature threshold layer are shown in Figure 17. Where areas of standing water are a significant source of confusion, they are eliminated by masking with the mapped evaporite minerals extent, retaining only those wet areas coincident with an evaporite crust.

The number of polygons and the total area for each threshold and their combinations is given in Table 8 for both the entire analysis area and within the defined study area.

**Table 8: Areas mapped by thresholds and their combinations**

	<b>Albedo Threshold 0.85 (evaporite)</b>	<b>Albedo Threshold 0.90 (evaporite)</b>	<b>Temperature (wet area)</b>	<b>Albedo 0.85 + Temp (current discharge)</b>	<b>Albedo 0.90 + Temp (current discharge)</b>
Analysis Mask					
No. of polygons	57,564	21,850	6,850	1,835	1,599
Area (Ha)	53,722	20,145	77,948	6,884	5,155
Study Area					
No. of polygons	15,056	4,159	1,115	603	391
Area (Ha)	11,523	3,174	12,524	1,517	1,076

The combined 0.85 PC1 and temperature thresholds resulted in 1,835 individual polygons totaling 6,884 hectares. The 0.90 PC1 and temperature threshold intersection produced 1,599 polygons covering a total of 5,155 hectares.

Due to the fine scale of the imagery not every point has been reproduced accurately in Figure 17. A more detailed view of the areas of interest is available in Appendix 2.

### 3.4 Accuracy evaluations

A series of images for each diffuse discharge area, both training and evaluation, are available in appendix 2. Each includes:

- true colour winter Landsat image
- principal component 1 (PC1) - without contrast stretch
- 0.85 PC1 albedo threshold
- 0.90 PC1 albedo threshold
- thermal band 10 winter - without contrast stretch
- temperature threshold
- intersection of 0.85 PC1 albedo threshold and temperature threshold

- intersection of 0.90 PC1 albedo threshold and temperature threshold

As stated previously, we were unable to carry out a quantitative accuracy assessment (such as errors of omission and commission) due to the lack of an adequate number of field-surveyed locations of diffuse discharge or verified mapped diffuse discharge extent. Table 9 outlines the evaluations we carried out on the two albedo thresholds, the temperature threshold and the combinations of these. The area (in hectares) for the Lewis and Gotch data and for each threshold and threshold combination are outlined in Table 10 (for both the training and evaluation data). Any polygon in the threshold data which intersects or is contained in the relevant training/evaluation dataset is chosen for the area calculation. Therefore the area calculated for the threshold data may contain some area outside the Lewis or Gotch data (i.e. where a threshold polygon extends beyond the training/evaluation data).

### 3.4.1 Albedo thresholds

The PC1 albedo thresholds are designed to identify areas of bright evaporite minerals. Comparisons with the Lewis diffuse discharge evaluation data and our two PC1 albedo thresholds are illustrated in Figure 18.

Freeling South shows about one quarter of the Lewis data was captured by our methodology, with results better in the southern section (Figure 18 and Table 10). The 0.85 threshold covers almost twice the area of 0.90 (Table 10) with both sitting within the Lewis mapped zone. In the Hermit Hill group, the evaporite area we identified follows the general distribution of the Lewis mapping, but with little actual overlap (Figure 18). Examination of the Landsat winter imagery shows the Lewis mapping is very fine and scattered compared to the pixel size of the Landsat imagery. The evaporite we detected is very bright compared to the area of the Lewis data. In the West Finnis Group our methodology has identified more potential evaporite along the south east of the Lewis evaluation data (Figure 18 and Table 10), and the Lewis data a little more in the central north, but otherwise there is good correspondence between the two data sets.

The diffuse discharge thresholds (PC1 albedo thresholds of 0.85 and 0.90) were also evaluated against the Gotch potential diffuse discharge evaluation polygons. The results can be seen in appendix 2 (Gotch polygon 1, 3, 5, 7, 9 and 10) and Table 10. These polygons were digitised freehand by Travis Gotch in ArcGIS and are a rough estimation of 'potential' diffuse discharge sites. Evaporite minerals are expected to be found somewhere within the polygon, but not necessarily within the entire polygon, as mentioned in section 2.4.2. All six polygons had some area mapped under the lower albedo threshold (0.85) (100% successful). Polygon 1 and 3 are in the north and the smaller of the evaluation polygons. Both have a scattering of small areas which fall within threshold 0.85, but polygon 3 does not have any in the higher threshold due to the fact the polygon is slightly off centre to the bright area in the Landsat imagery. Polygon 5 has a negligible area within the 0.85 threshold and does not look like a bright area in the Landsat imagery, while polygon 7 is very well defined by both thresholds. The final two evaluation areas are beside one another.

The evaporite detection is fragmented in both and only the outer section of polygon 9 is highlighted by threshold 0.90 (as was expected by Trevor Gotch). In all cases the evaporite detection matches the 'white' areas in the true colour Landsat imagery.

**Table 9: Data used in evaluation of diffuse discharge mapping**

Name	Year	Data type	Albedo Threshold 0.85 (evaporite)	Albedo Threshold 0.90 (evaporite)	Temperature (wet area)	Albedo 0.85 + Temp (current discharge)	Albedo 0.90 + Temp (current discharge)
Freeling South	2011	DD	X	X	-		
Hermit Hill Group (HHC)	2011	DD	X	X	-		
West Finniss Group (HHC)	2011	DD	X	X	-		
Freeling	2011	NSMI	-	-	X		
Francis Swamp	2001	Thermal	-	-	X		
Francis Swamp	2009	NSMI	-	-	X		
Hermit Hill Complex	2011	NSMI	-	-	X		
Gotch polygon 1	2015	Sketch	X	X	X	X	X
Gotch polygon 3	2015	Sketch	X	X	X	X	X
Gotch polygon 5	2015	Sketch	X	X	X	X	X
Gotch polygon 7	2015	Sketch	X	X	X	X	X
Gotch polygon 9	2015	Sketch	X	X	X	X	X
Gotch polygon 10	2015	Sketch	X	X	X	X	X
Gotch Springs Data	Various	Point Shapefile	X	X	X	X	X

**Table 10: Comparison of the area (hectares) of both the training and evaluation data with the area of mapped diffuse discharge in the same vicinity**

Please use this Table in conjunction with the relevant maps (Figures 18 and 19 and Appendix 2)

Note: Any polygon in the mapped diffuse discharge which intersects or is contained in the relevant training/evaluation dataset is chosen. Therefore the area calculated for the threshold data may contain some area outside the Lewis or Gotch data (i.e. where a threshold polygon extends beyond the training/evaluation data)

\* Hermit Hill Group (HHC) - first figure is actual intersection with Lewis data; second figure is data in the general vicinity

\*\* This mapping shows a range of surface temperatures, rather than a delineated zone of near-surface moisture, hence an area is not calculated.

Name	Year	Data type	Lewis or Gotch (Ha)	0.85 (evaporite) (Ha)	0.90 (evaporite) (Ha)	Temp (wet area) (Ha)	0.85 + Temp (current discharge) (Ha)	0.90 + Temp (current discharge) (Ha)
Training Data								
Hermit Hill Complex	2009	Diffuse Discharge	234	386	228	47	64	49
Hermit Hill Complex	2009	NSMI	176	n/a	n/a	213	62	45
Gotch polygon 2	2015	Sketch	64	39	32	48	36	32
Gotch polygon 4	2015	Sketch	228	18	4	0	0	0
Gotch polygon 6	2015	Sketch	1,831	491	364	526	373	309
Gotch polygon 8	2015	Sketch	43	19	12	14	10	8
Gotch polygon 11	2015	Sketch	605	39	250	618	331	244
Gotch Springs Data	Various	3 Point Shapefiles	n/a	n/a	n/a	n/a	n/a	n/a
Evaluation Data								
Freeling South	2011	Diffuse Discharge	30	8	5	4	2	2
Hermit Hill Group (HHC)	2011	Diffuse Discharge	9	5/19*	1/11*	35	1	0.1
West Finnis Group (HHC)	2011	Diffuse Discharge	24	57	28	72	23	12
Freeling South subset	2011	NSMI	35	n/a	n/a	4	2	2
Francis Swamp	2001	Thermal**	-	n/a	n/a	3166	2197	1773
Francis Swamp	2009	NSMI	5,031	n/a	n/a	3,149	2,191	1,771
Hermit Hill Complex	2011	NSMI	611	n/a	n/a	213	63	48
Gotch polygon 1	2015	Sketch	37	9	3	25	6	2
Gotch polygon 3	2015	Sketch	47	7	0.2	0	0	0
Gotch polygon 5	2015	Sketch	1,567	13	0	0	0	0
Gotch polygon 7	2015	Sketch	73	86	71	77	67	61
Gotch polygon 9	2015	Sketch	611	45	17	71	27	15
Gotch polygon 10	2015	Sketch	2,783	441	178	327	183	127
Gotch Springs Data	Various	3 Point Shapefiles	n/a	n/a	n/a	n/a	n/a	n/a

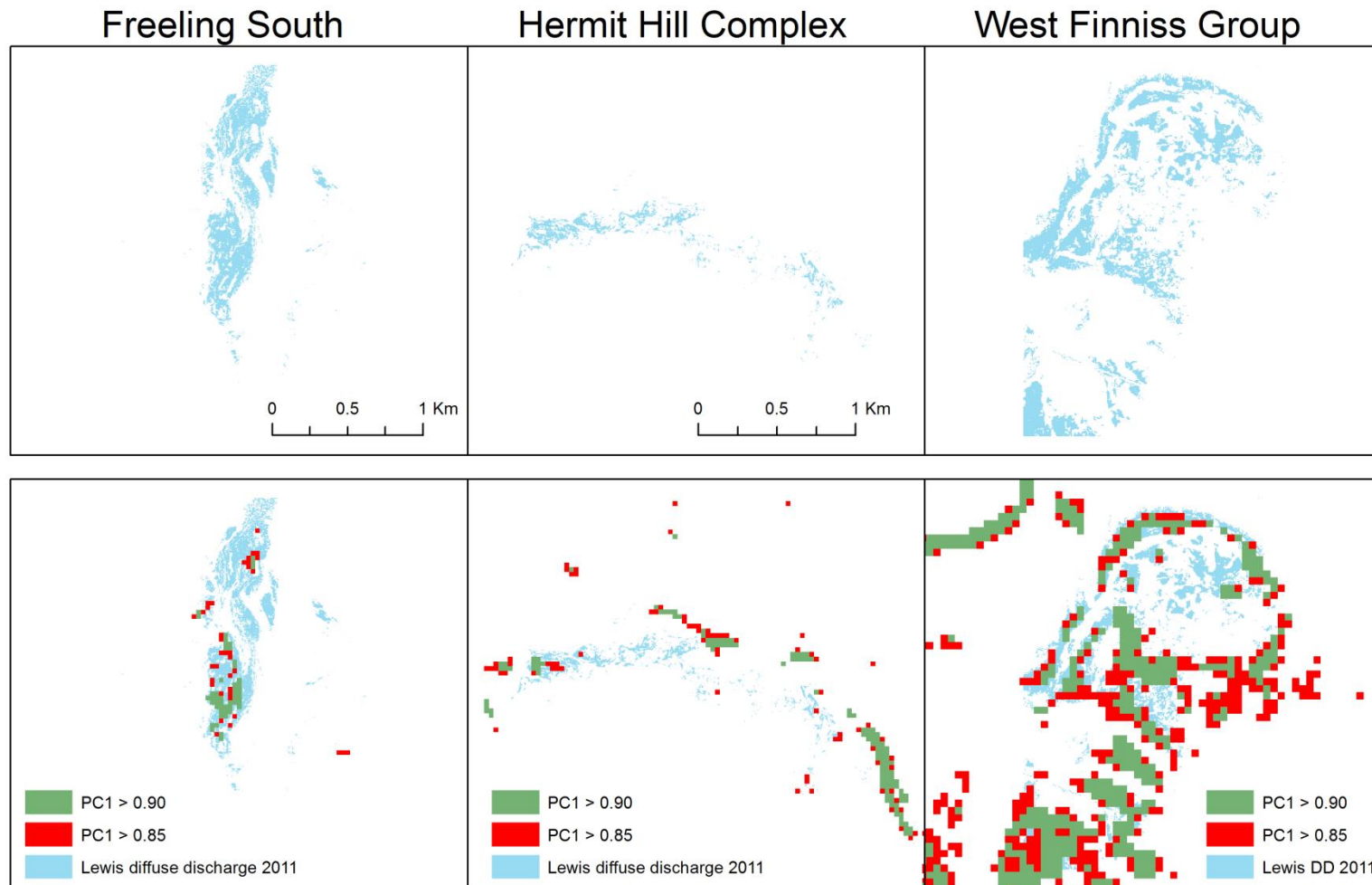


**Figure 18: Comparison of Lewis diffuse discharge evaluation data with PC1 albedo thresholds 0.85 and 0.90 (a) Freeling South 2011 (b) Hermit Hill Group 2011 (c) West Finnis Group 2011**

*PC1 threshold 0.85 includes both the green and red areas. PC1 threshold 0.90 is the green areas only*



### **3.4.2 Temperature thresholds**

The temperature thresholds (a separate threshold for each Landsat date/path) highlight areas that are cooler than the surrounding landscape. This is often an indication that the ground is wet.

Figure 19 compares the Lewis evaluation NSMI and ASTER temperature data with our temperature thresholds (The Hermit Hill Complex 2011 NSMI which falls in Landsat path 099; Freeling South 2011 NSMI, Francis Swamp 2009 NSMI and 2001 ASTER temperature data which fall in Landsat path 100). Results of the areas (hectares) identified by our thresholds are available in Table 10. The 2011 period was wetter than 2009, which is reflected in the Freeling South 2011 NSMI data (near surface moisture index). This difference is also highlighted by the 2009 and 2011 Hermit Hill Complex NSMI (Figure 5b and Figure 5c). There is far more moisture indicated in both these areas in 2011 than we have identified as cold (potentially wet) areas from the winter Landsat imagery from 2014. However the two Lewis datasets for Francis Swamp (2001 ASTER temperature and 2009 NSMI) fit well with our temperature threshold. The Francis Swamp data was supplied as a range of values, with many of the very low values occupying the speckle around the swamp. We were not supplied a threshold value for this dataset.

In the Gotch evaluation data, almost all of polygon 1 and 7, but none of polygon 3 or 5, fall within the low temperature threshold (appendix 2). The low temperature areas in polygons 9 and 10 are fragmented, covering approximately 11% of each polygon (Table 10). As expected, this does not include the inner polygon 9.

### **3.4.3 Combined albedo and temperature thresholds**

The combined albedo and temperature thresholds are a function of how successful the individual thresholds were at identifying bright and cold areas. This has the potential to identify those areas which currently have active diffuse discharge.

The results can be seen for each area, both Lewis and Gotch training and evaluation data, in appendix 2 and Table 10. A number of the Gotch polygons do not appear to be currently active areas of diffuse discharge but were probably in the past (polygons 3 and 4). Polygon 5 has only a few pixels in the lower albedo threshold and none in the temperature threshold. The Landsat imagery looks quite different from the other Gotch polygons and does not appear to contain bright evaporite minerals. This would suggest that polygon 5 is unlikely to be, or have been, an area of diffuse discharge. All other areas have at least some areas of active diffuse discharge (i.e. bright and potentially damp/wet (the southern end of Freeling South, almost all of Francis Swamp, sections at the Hermit Hill complex, a large portion of Gotch polygon 2, 7 and 11, and portions of polygon 1, 6, 8, 9 and 10).

### **3.4.4 Gotch spring vent data**

An examination of where the Gotch spring vent locations intersect the albedo and temperature thresholds, and the combination thereof, was also undertaken. As spring vents and diffuse discharge are often found in association, but one can be found without the other,

we can only use this information as an indication that our mapping methodology is identifying likely areas of diffuse discharge.

The following analysis only considers the 0.85 PC1 albedo threshold. The other results are available in Table 11.

In the GAB Springs RTK survey group of 2,866 vents over half are within, or less than, 50 metres from mapped evaporite (with the 0.85 threshold). Over 70 percent are within 100 metres of mapped evaporite and less than two percent (45 vents) are more than 500 metres away, including 12 in the WDS spring group and 9 ATS, 6 LSS and 5 NHS vents. When the temperature threshold is added to the 0.85 albedo threshold, over 30 percent fall within 50 metres of wet evaporite areas. Over 25% (724 vents) are more than 500 metres distant, including 260 HHS, 93 NHS, 75 WDS, 35 HOW, and 23 EFN vents. These Figures would suggest that our methodology works well.

In the non RTK survey group however, few of the 63 vents are within 100 metres from the evaporite mapped with the 0.85 albedo threshold. Forty six percent are more than 500 metres away including the Lake Cadibarrawirracanna, Giddi-Giddinna and Oolgilima vents.

The estimated locations for the 5 Toodina vents were between 50 and 500 metres away from any of identified diffuse discharge areas.

A breakdown by the flow attribute for the RTK survey group is also given in Table 12. Of the 46% (92) Freewater and Tail vents which are more than 100 metres distant from mapped evaporite in the 0.85 threshold, 33 are in the NHS group and 15 in the FFS spring group. For the 23 saturated ground vents more than 100 metres from mapped 0.85 threshold evaporite, 8 are in NHS and 4 each in NLS and POS.

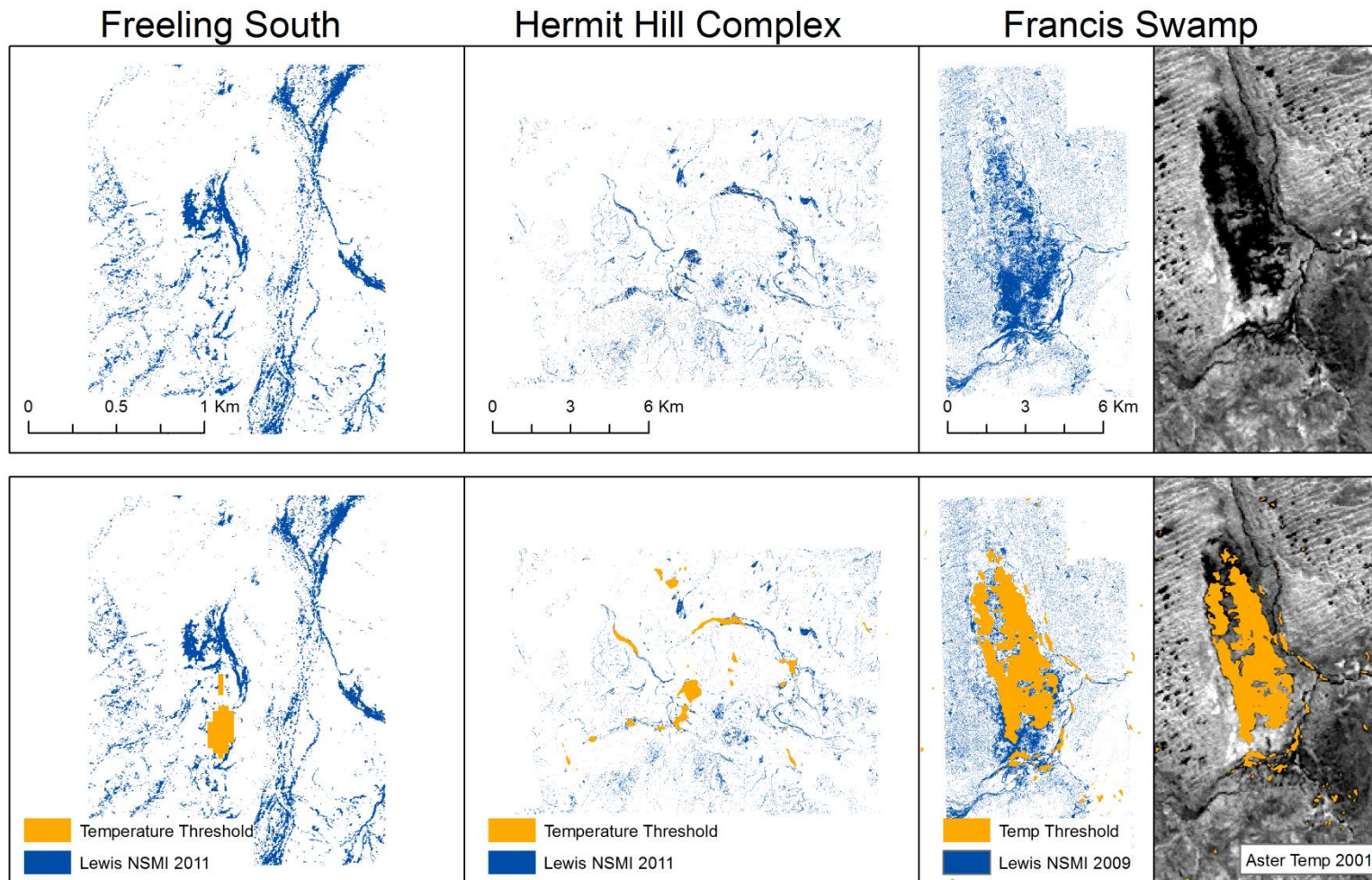


Figure 19: Comparison of Lewis NSMI and ASTER Temperature evaluation data with temperature thresholds (a) Freeling South NSMI 2011 (b) Hermit Hill Complex NSMI 2011 (c) Francis Swamp NSMI 2009 (d) Francis Swamp ASTER Temperature 2001

**Table 11: Percentage of vents within a range of distances from areas of diffuse discharge mapped by the albedo and temperature thresholds and their combinations**

Distance to closest feature	Albedo Threshold 0.85 (evaporite)	Albedo Threshold 0.90 (evaporite)	Temperature (wet area)	Albedo 0.85 + Temp (current discharge)	Albedo 0.90 + Temp (current discharge)
metres	%	%	%	%	%
GAB Springs RTK: 2,866 vents					
0	17.2	9.8	40.0	10.5	5.8
< 10	6.9	5.2	2.9	4.4	3.5
< 50	28.8	24.5	10.2	17.0	16.4
< 100	19.5	19.5	8.2	11.9	12.7
< 500	26.0	36.4	23.6	30.9	32.4
> 500	1.6	4.6	15.2	25.3	29.2
GAB Springs Non RTK: 63 vents					
0	3.2	1.6	4.8	1.6	1.6
< 10	1.6	0.0	0.0	0.0	0.0
< 50	4.8	3.2	1.6	1.6	1.6
< 100	4.8	3.2	0.0	1.6	1.6
< 500	39.7	17.5	14.3	4.8	4.8
> 500	46.0	74.6	79.4	90.5	90.5
Toodina location estimate: 5 vents					
0	0.0	0.0	0.0	0.0	0.0
< 10	0.0	0.0	0.0	0.0	0.0
< 50	0.0	0.0	0.0	0.0	0.0
< 100	40.0	40.0	0.0	0.0	0.0
< 500	60.0	60.0	0.0	0.0	0.0
> 500	0.0	0.0	100.0	100.0	100.0

**Table 12: Percentage of vents per flow attribute within a range of distances from areas of diffuse discharge mapped by the albedo and temperature thresholds and their combinations for the GAB Springs RTK vents**

Distance to closest feature	Albedo Threshold 0.85 (evaporite)	Albedo Threshold 0.90 (evaporite)	Temperature (wet area)	Albedo 0.85 + Temp (current discharge)	Albedo 0.90 + Temp (current discharge)
metres	%	%	%	%	%
Damp: 625 vents					
0	28.2	14.7	60.2	26.1	13.9
< 10	10.9	9.3	1.1	9.6	8.2
< 50	34.4	33.1	7.0	26.7	29.4
< 100	11.4	17.8	5.4	8.0	14.9
< 500	14.9	21.9	14.2	16.0	19.4
> 500	0.3	3.2	12.0	13.6	14.2
Dry: 70 vents					
0	25.7	17.1	47.1	24.3	15.7
< 10	5.7	5.7	1.4	2.9	5.7
< 50	34.3	28.6	5.7	22.9	20.0
< 100	12.9	14.3	4.3	5.7	12.9
< 500	17.1	24.3	28.6	24.3	22.9
> 500	4.3	10.0	12.9	20.0	22.9
Extinct: 410 vents					
0	46.3	28.3	36.6	20.5	12.4
< 10	10.2	7.3	4.4	7.1	4.9
< 50	28.5	27.6	10.5	21.7	21.7

< 100	9.3	17.1	13.9	14.9	15.1
< 500	5.4	18.8	33.2	34.1	39.8
> 500	0.2	1.0	1.5	1.7	6.1
Freewater: 164 vents					
0	4.9	1.2	58.5	4.9	1.2
< 10	6.1	6.7	2.4	5.5	6.1
< 50	47.0	36.6	5.5	40.9	34.8
< 100	21.3	20.1	4.3	14.0	17.1
< 500	18.9	28.7	12.8	16.5	21.3
> 500	1.8	6.7	16.5	18.3	19.5
Freewater and Tail: 195 vents					
0	2.1	0.5	15.4	1.5	0.5
< 10	4.1	3.6	0.5	2.1	1.5
< 50	27.2	12.8	9.2	8.7	7.7
< 100	19.5	14.9	7.7	13.3	9.2
< 500	41.0	45.6	24.1	22.6	25.6
> 500	6.2	22.6	43.1	51.8	55.4
Saturate/Saturated: 73 vents					
0	16.4	11.0	20.5	9.6	6.8
< 10	5.5	5.5	0.0	2.7	2.7
< 50	37.0	28.8	11.0	12.3	11.0
< 100	9.6	15.1	5.5	6.8	5.5
< 500	31.5	30.1	20.5	17.8	23.3
> 500	0.0	9.6	42.5	50.7	50.7
Blank: 1,329 vents					
0	6.5	3.7	33.6	1.4	0.7
< 10	4.7	2.7	3.8	1.5	0.7
< 50	23.5	19.2	12.4	9.2	7.8
< 100	27.2	22.1	8.6	13.0	11.3
< 500	36.4	49.3	26.3	41.1	39.7
> 500	1.8	3.0	15.3	33.9	40.0

## 4 Discussion and recommendations

The methodology presented here uses free Landsat satellite data, and could in principle be applied elsewhere to detect similar diffuse discharge zones. If this method is applied elsewhere, variation in soil colour or spring geomorphology would make accuracy assessment advisable.

White et al. 2013 chose to study Freeling, Francis and Hermit Hill because they cover the range of spring forms present in this part of the GAB. The relative difficulty of mapping wet and bright areas at a number of sites (Gotch polygons 3, 4, and 5) may indicate that the type of spring represented by them may be consistently problematic for the methods developed in this report. The otherwise generally good performance of our methods seems to indicate that Gotch polygon 5 in particular is more likely to be an outlier, and we suggest that the methods should detect some or most of all areas of diffuse discharge in the region. However, the results of this analysis, as well as the Lewis and Gotch data, should be quantitatively assessed in the field.

For the purposes of this analysis, we have had to make the assumption that there was no change in wet areas between the time the training data analysis was performed, and the time our analysis was performed. However, we know from this study that temperature can change significantly between winter and summer. Where possible we used the 2009 data for training, which was drier than 2011. This could be a potential issue for future analysis. We recommend that further investigation be undertaken to develop a more robust temperature/wetness index.

With further research, it should be possible to develop a spatially and temporally generalisable diffuse discharge index by combining the quantitative temperature method from this project with an objective brightness measure, to remove the dependence on field training data. Further investigation will determine which thresholds are most appropriate, depending on the purpose of the exercise.

The results of this analysis should be incorporated in future assessments of the GAB water balance. The analysis in this report could be repeated periodically to monitor changes in diffuse discharge from the GAB.

## 4.1 Recommendations

- The results of this analysis, as well as the Lewis and Gotch data, should be quantitatively assessed in the field.
- Further investigation will determine which thresholds are most appropriate, depending on the purpose of the exercise.
- Repeat the analysis periodically to monitor the health of the GAB.
- We recommend that winter imagery be used for future analysis, as there is greater contrast between areas of evaporite and exposed bright soils in winter.
- If applied elsewhere, variation in soil colour or spring geomorphology would make accuracy assessment advisable.
- The results of this analysis should be used to better understand the water balance of the GAB.
- We recommend that further investigation be undertaken to develop a more robust temperature/wetness index.
- With further research, it should be possible to develop a spatially and temporally generalisable diffuse discharge index by combining the quantitative temperature method from this project with an objective brightness measure, to remove the dependence on field training data.

## References

Department of the Environment (2012). National Partnership Agreement on Coal Seam Gas and Large Coal Mining Development. Australian Government. Available at <https://www.ehp.qld.gov.au/management/impact-assessment/pdf/partnership-agreement.pdf>

Bureau of Meteorology (2015). Climate Data Online, Bureau of Meteorology. Available at <http://www.bom.gov.au/climate/data/index.shtml>

Department of the Environment (2012). National Partnership Agreement on Coal Seam Gas and Large Coal Mining Development. Australian Government. Available at <https://www.ehp.qld.gov.au/management/impact-assessment/pdf/partnership-agreement.pdf>

Gotch, T.B. (2013). Spatial Survey of Springs. In *Volume IV: Spatial Survey and Remote Sensing of Artesian Springs of the Western Great Artesian Basin*. eds M. M. Lewis, D. C. White and T. B. Gotch pp. 24-69. National Water Commission, Canberra.

Ryan, J. (2014). Multidisciplinary Synthesis: A Joint Remote Sensing and Geophysical Approach to the Analysis of Artesian Springs Discharge in the Great Artesian Basin. Honours dissertation, School of Earth and Environmental Sciences, The University of Adelaide.













Schofield, B. (2014). Identifying Acid Sulphate Soils using Hyperspectral Signatures and Imagery, Honours dissertation, School of Earth and Environmental Sciences, The University of Adelaide.

USGS (2013). Using the USGS Landsat 8 Product. U.S. Geological Survey. Available at [http://landsat.usgs.gov/Landsat8\\_Using\\_Product.php](http://landsat.usgs.gov/Landsat8_Using_Product.php)

White D. C., Gotch T. B., Alaak Y., Clark M., Ryan J. and Lewis M. M. (2013). Characterising spring groups. In *Volume IV: Spatial Survey and Remote Sensing of Artesian Springs of the Western Great Artesian Basin*. eds M. M. Lewis, D. C. White and T. B. Gotch pp. 24-69. National Water Commission, Canberra.



## Appendix 1. Monthly rainfall at Coober Pedy Airport 2013 and 2014 (mm)

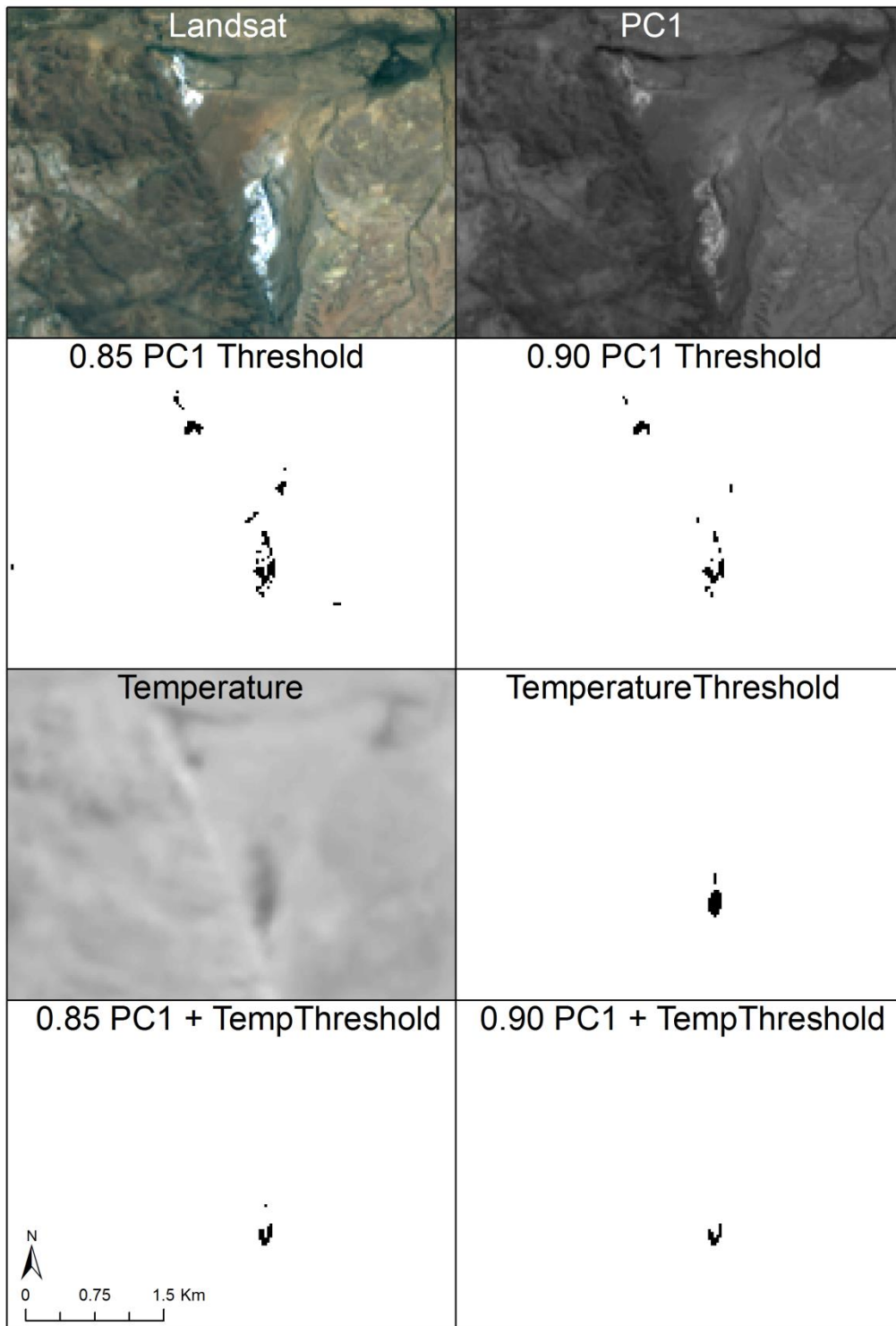
2013	Jan	Feb	Mar	Apr	May	Jun	Jul	Aug	Sep	Oct	Nov	Dec
<b>Graph</b>												
<b>1st</b>	0	0	0	0.2	0	24.0	0	0	0	0.6	0	8.8
<b>2nd</b>	0	0	0	0	0	0	0	0	0	0	0	1.0
<b>3rd</b>	0	0	0	0	0	0	0	0	0	0	0	0
<b>4th</b>	0	0	0	0	0	0	0	0	0	0	0	2.4
<b>5th</b>	0	0	0	0	0	0.2	0	0	0	0	0	0
<b>6th</b>	0	0	0	0	0	1.8	0	0	0	0	0	0
<b>7th</b>	0	0	0	0	0	0	0	0	0	0	0	0
<b>8th</b>	0	0	0.2	0	0	0.2	0	0	0	0	0.8	0
<b>9th</b>	0	0	24.8	0	0	0	0	0	0	0	0.2	0
<b>10th</b>	0	0	0	0	0	0	0	0	0	0	0	0
<b>11th</b>	0	0	0	0	0	12.8	0	0	0	0	0	0
<b>12th</b>	0	0.4	0	0	10.4	0	0	0	0	0	0	0
<b>13th</b>	0	0	0	0	0	0	0	0	0	0	0	0
<b>14th</b>	0	0	0	0	0	0	0	0	0	0	0	0
<b>15th</b>	0	0	0	5.2	0	0.2	0	0	0	0	0	0
<b>16th</b>	0	0	0	0.2	0	0	0	0	0	0	0	0
<b>17th</b>	0	0	0	0	0	0	0	0	0	0	0	0
<b>18th</b>	0	0	0	0	0	0	1.2	0	0	0	0	0
<b>19th</b>	0	0	0	0	0	0	0	0	0	0	0	0
<b>20th</b>	0	0	0	0	0	0	0.2	0	0	0	0.2	0
<b>21st</b>	0	0	0	0	7.6	0	0.6	0	0	0	0.2	0.8
<b>22nd</b>	0	0.2	0	0	6.8	0	0	0	0	2.4	0	0
<b>23rd</b>	0	0	0	0	0	0	0	0	0	0	0	1.2
<b>24th</b>	0	0	0	0	0	0	0	0	0	0	0	0.2
<b>25th</b>	0	0	0	0	0	0	0	0	0	0	0	0
<b>26th</b>	0	0	0	0	0	0.8	0	0	0	0	0	0
<b>27th</b>	0	4.6	0	0	0	3.2	0	0	0	0	0	0
<b>28th</b>	0	2.6	5.0	0	0	0.2	0	0	0	0	0	0
<b>29th</b>	0		0.2	0	0	0	0	0	0	0	0	0
<b>30th</b>	0		1.0	0	0	0	0	0	0	0	0	0
<b>31st</b>	0		6.8		3.0		0	1.4		0		0
<b>Highest Daily</b>	0.0	4.6	24.8	5.2	10.4	24.0	1.2	1.4	0.0	2.4	0.8	8.8
<b>Monthly Total</b>	0.0	7.8	38.0	5.6	27.8	43.4	2.0	1.4	0.0	3.0	1.4	14.4

Source: BOM 2015 <http://www.bom.gov.au/climate/data/index.shtml>

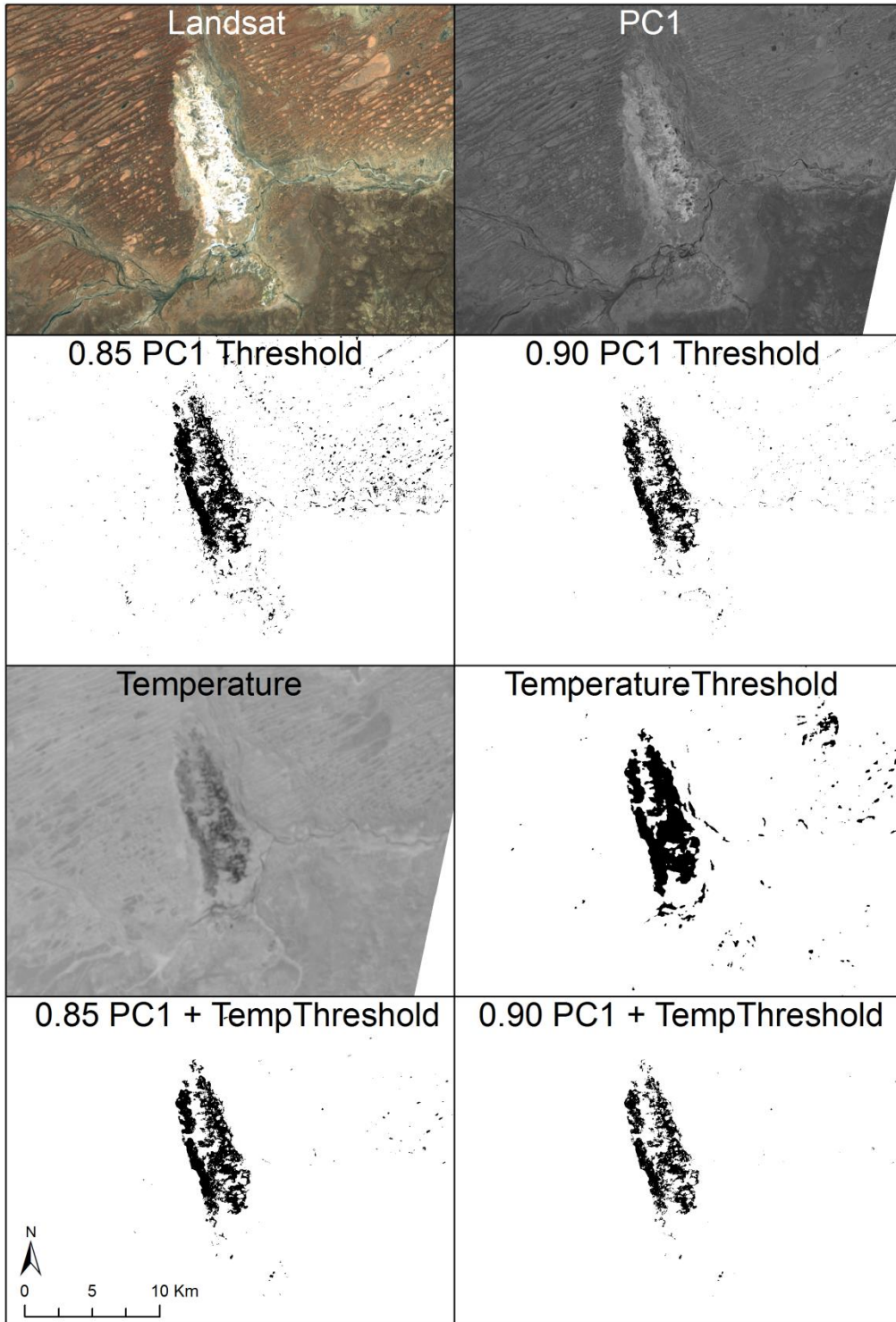
2014	Jan	Feb	Mar	Apr	May	Jun	Jul	Aug	Sep	Oct	Nov	Dec
Graph												
1st	0	0	0	0	0	0	0	0	0	0	4.0	0
2nd	0	0	0	0.6	0	0	0	0	0	0	0	0
3rd	0	0	0	20.2	0.4	0	0	0	0	0	0	0.4
4th	0	0	0	4.8	6.8	0	0	0	0	0	0	0
5th	0	0	0	0	0	0	0	0	0	0	0	0
6th	0	0	0	0	0.2	0	0	0	0	0	0	0
7th	0	0	0	0	0	0	0	0	0	0	0	0
8th	0	0	0	0.8	0	0	0	0	0	0	0	0
9th	0	0	0	8.0	4.6	0	0	0	0	0	0	0
10th	0	0	0	115.0	0.4	0	0	0	0	0	0	0
11th	0	0	0	0	0	0	0	0	0	0	0	0
12th	0	2.2	0	0	0	0	0	0	0	0	0	0
13th	0	0	0	0	0	0	0	0	0	0	0	0
14th	0	1.8	0	0	0	0	0.4	0	0	0	0	0
15th	0	21.0	0	0	0	0	0.2	0.8	0	0	0.4	0
16th	0	0	0	0	0	0	0	0	0	0	0.4	0
17th	0	0	0	0	0	0	0	0	0	0	0	0
18th	0	0	0	0	0	0	0	0	0	0	0	0
19th	0	0	0	0	0	0	0	0	0	0	0	0
20th	0	0	0	0	0	0	0	0	0	0	5.6	0
21st	0	0	0	0	0	0	0	0	0.2	0	0.8	0
22nd	0	0	0	0	0	0	0	0	0	0	0	2.2
23rd	0	0	0	0	1.0	0	1.0	0	0	0	0	0
24th	0	0	0	0	0.2	0	1.4	0	0	0	0.4	0
25th	0	0	0	0	0	0.2	0	0	0	0	0	0
26th	0	0	0	0	0	0	0	0	0	0	0	0
27th	0	0	0	0	0.8	0	0	0	0	0.2	0	0
28th	0	0	0	0	0.2	0	0	0	0	0	0	0
29th	0		0	9.0	0	0	0	0	0	0	0	0
30th	0		0	3.2	0	0	0	0	0	0	0	0
31st	0		0		0		0	0		0		0
Highest Daily	0.0	21.0	0.0	115.0	6.8	0.2	1.4	0.8	0.2	0.2	5.6	2.2
Monthly Total	0.0	25.0	0.0	161.6	14.6	0.2	3.0	0.8	0.2	0.2	11.6	2.6

Source: BOM 2015 <http://www.bom.gov.au/climate/data/index.shtml>

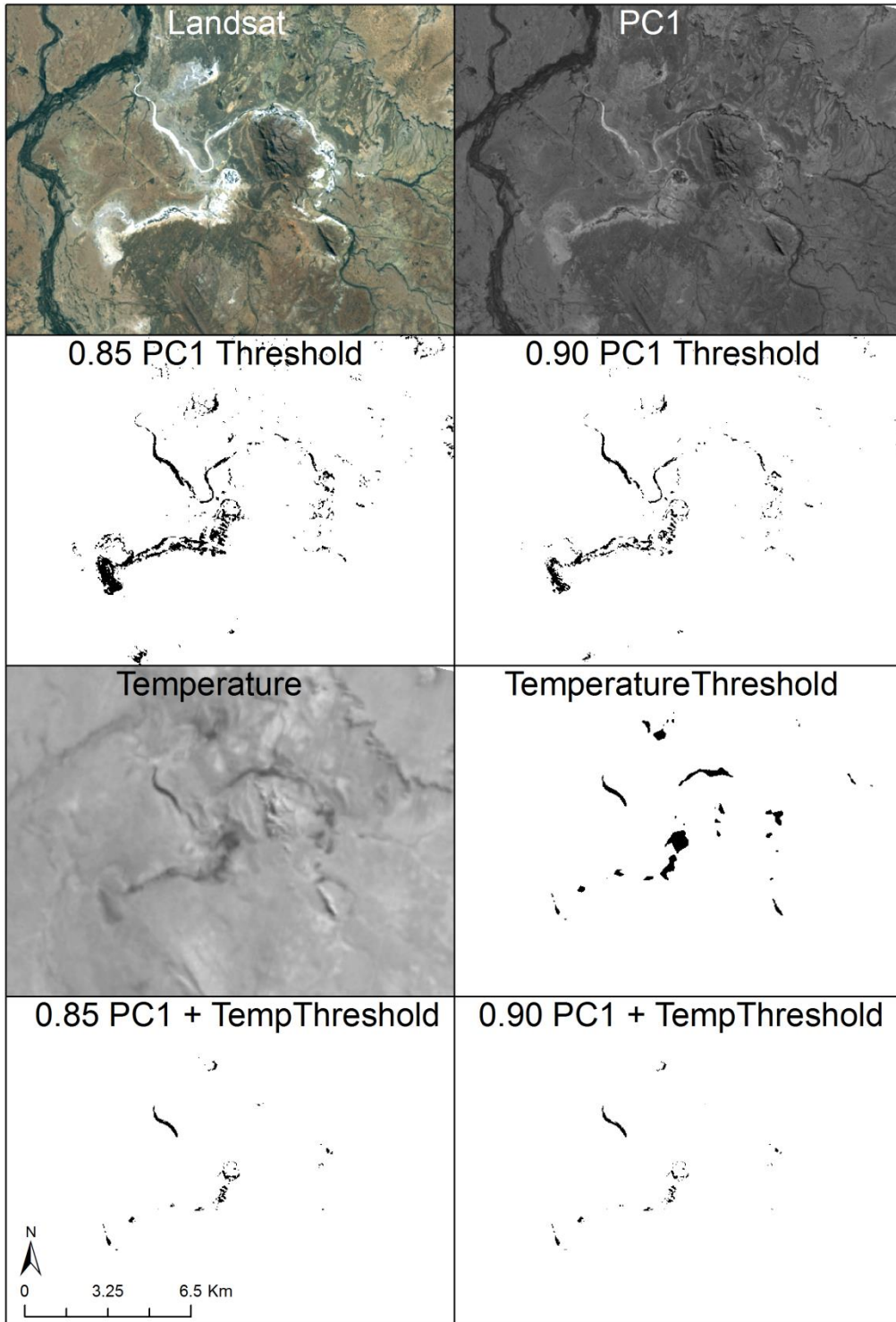
## Appendix 2. Enlargements of areas of interest



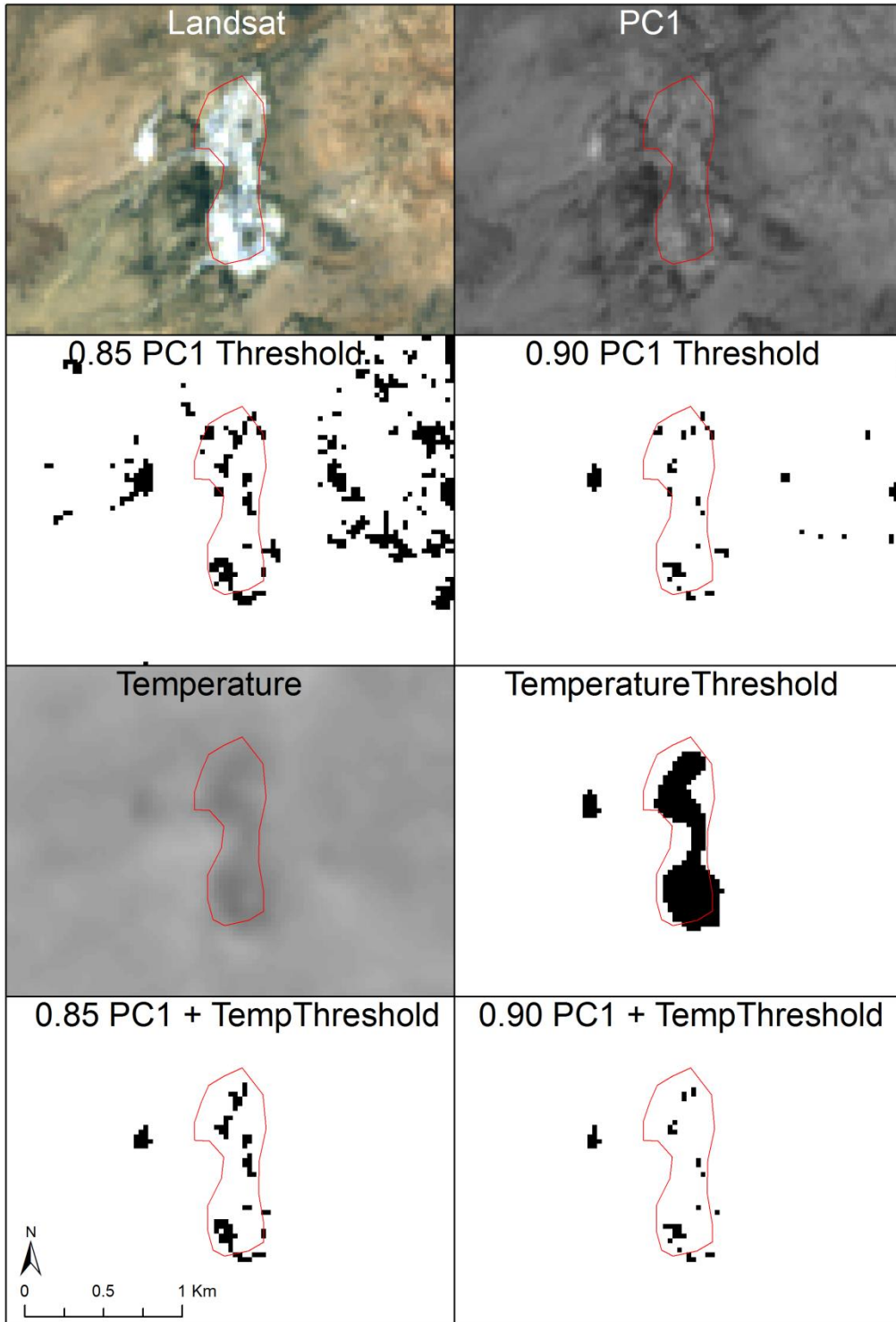
Freeling South



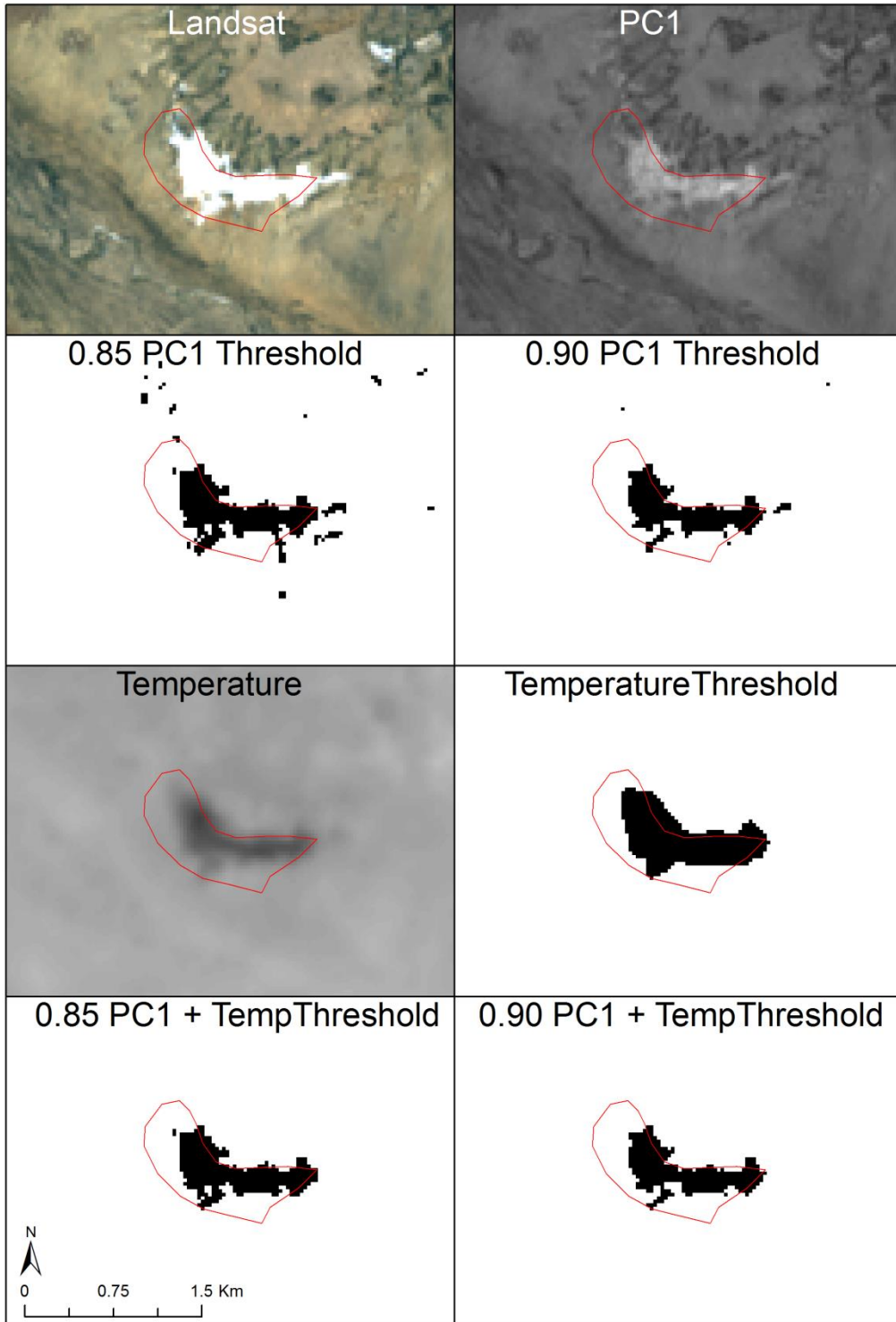
**Francis Swamp**



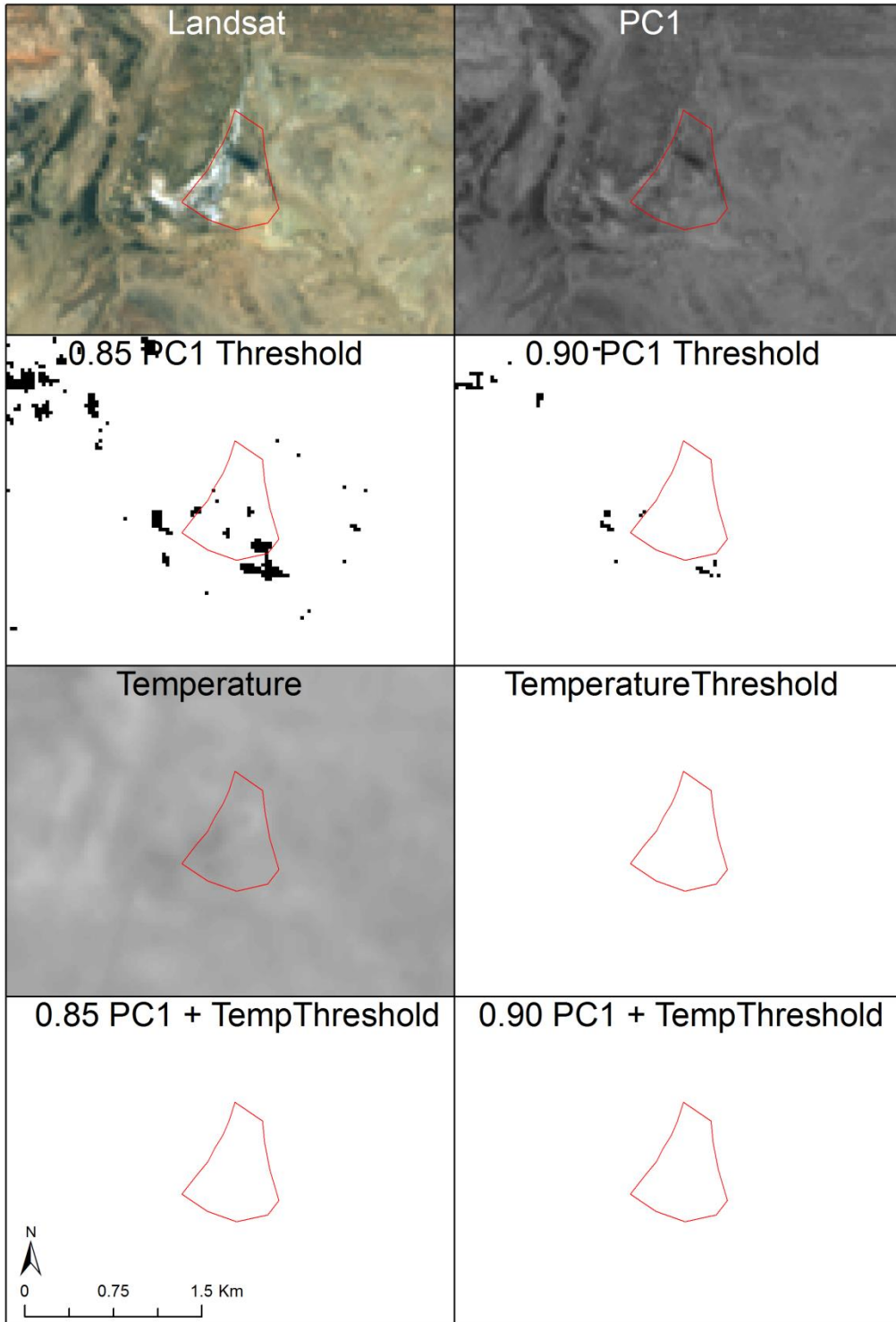
**Hermit Hill Complex**



Gotch polygon 1

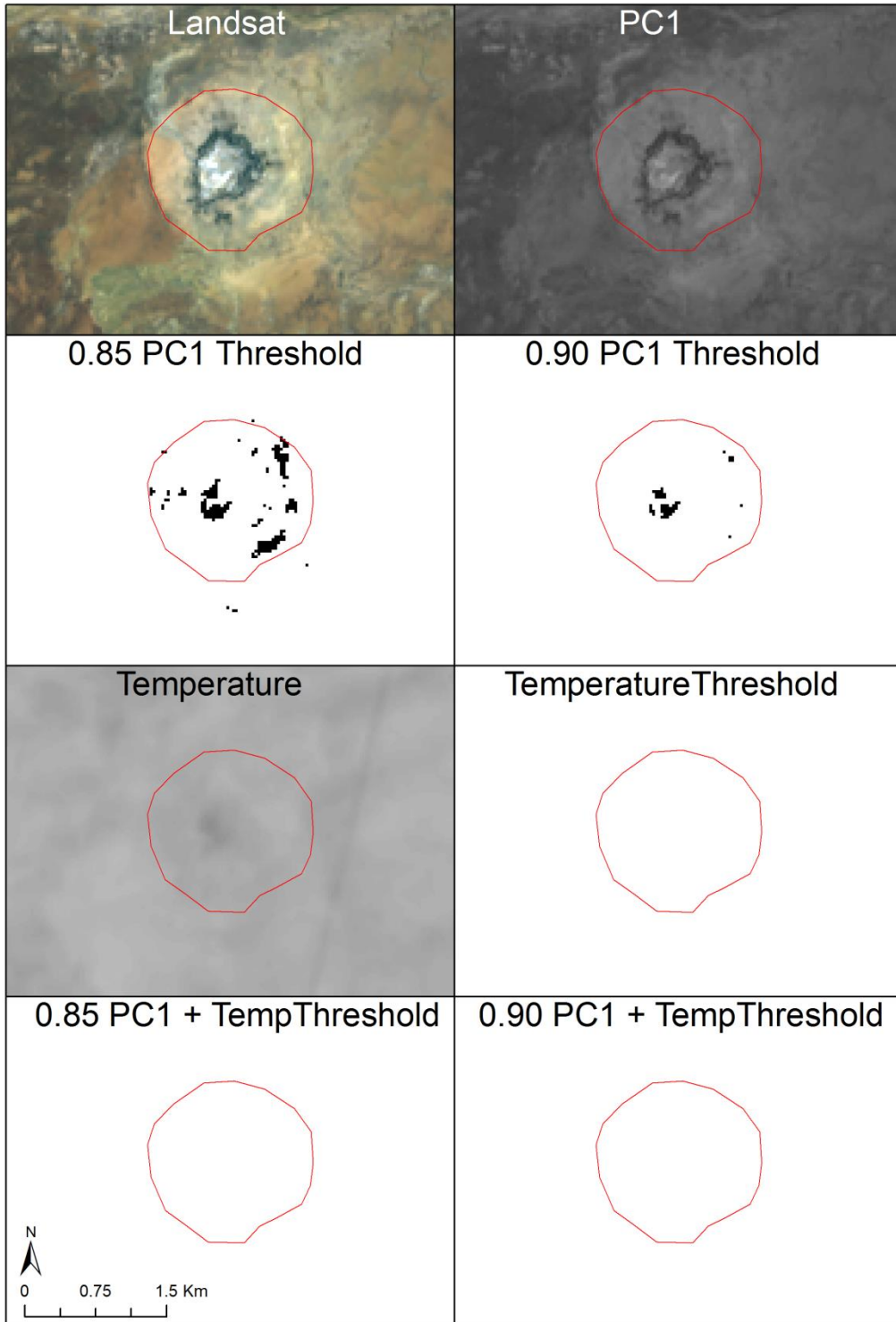


Gotch polygon 2

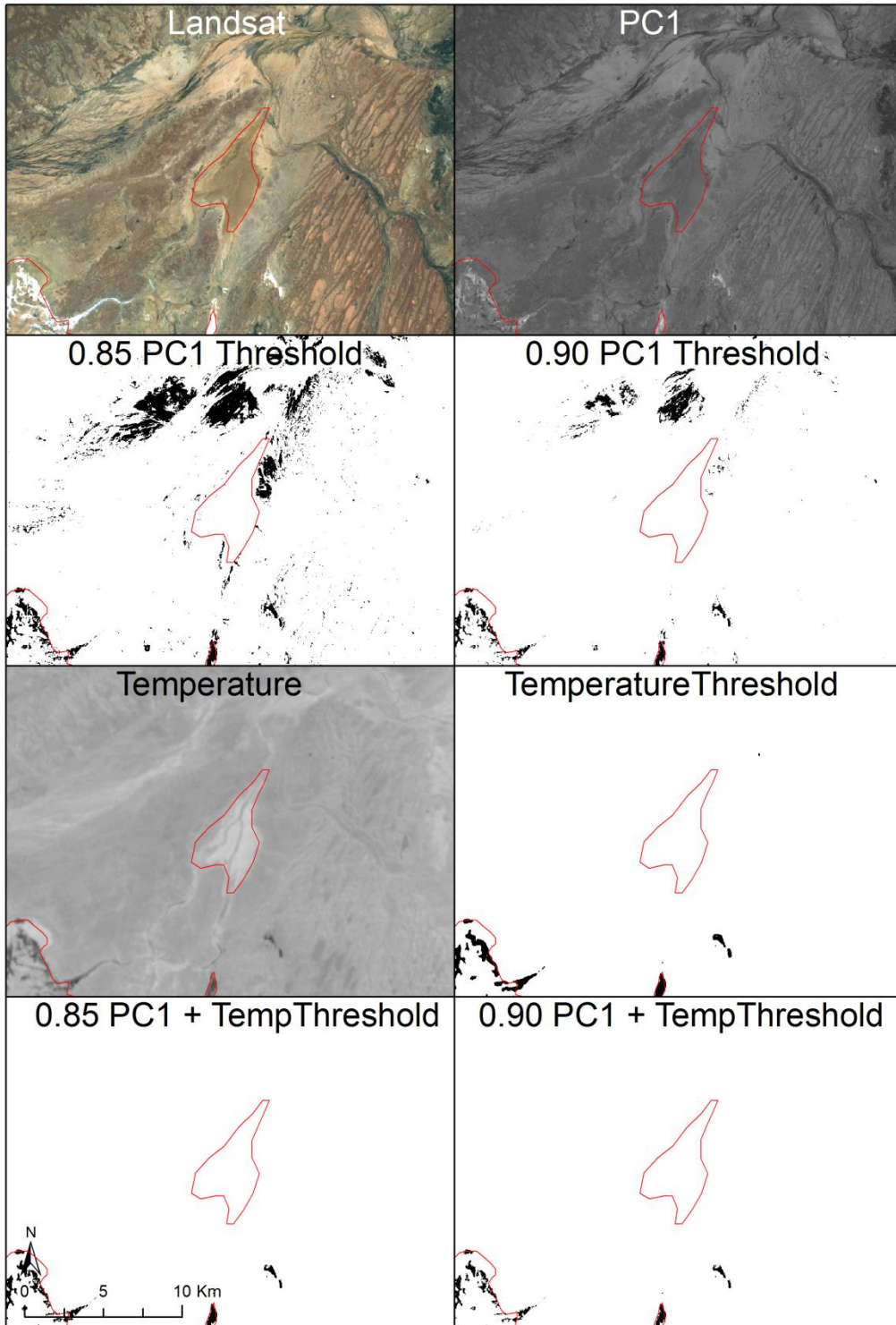


Gotch polygon 3

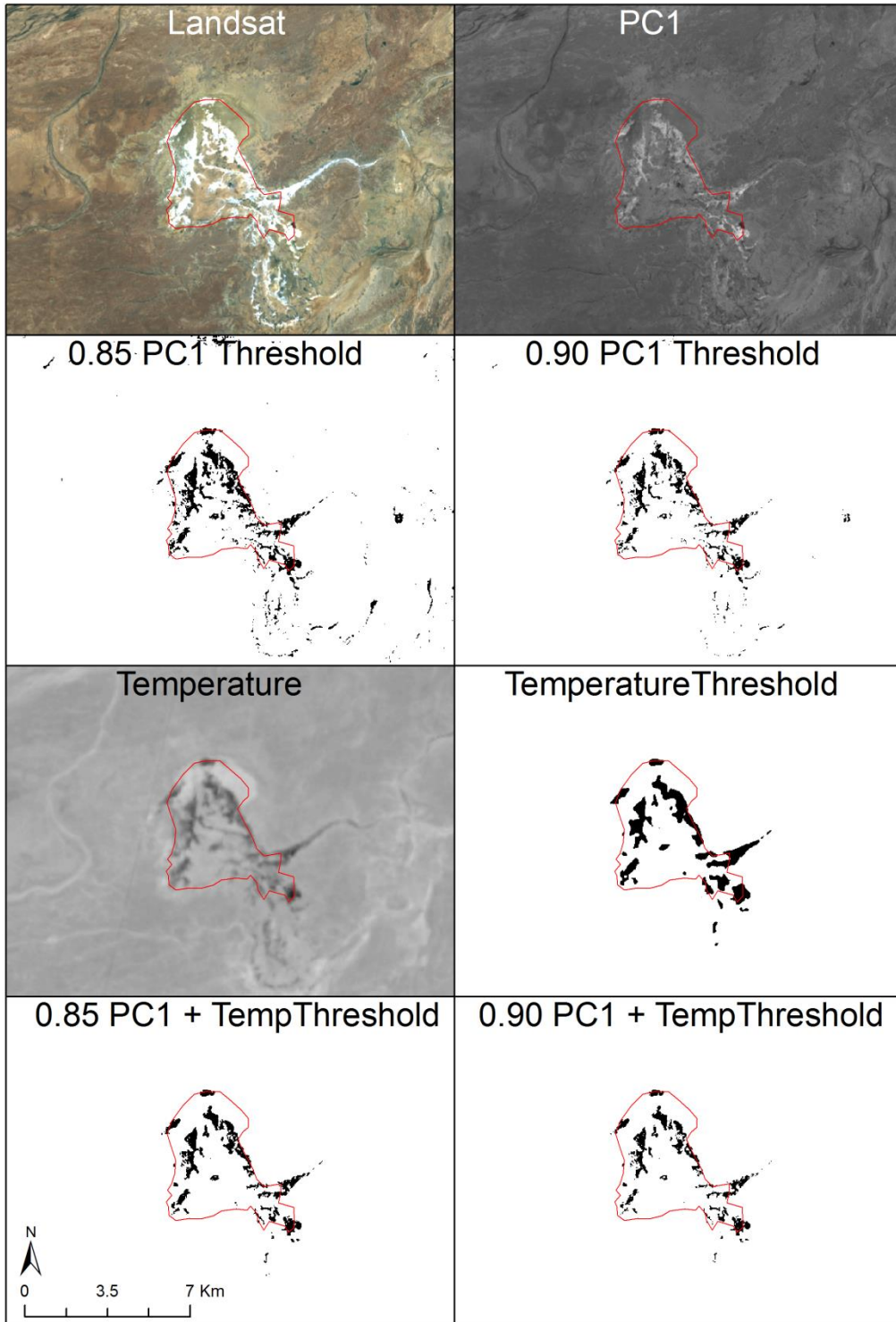




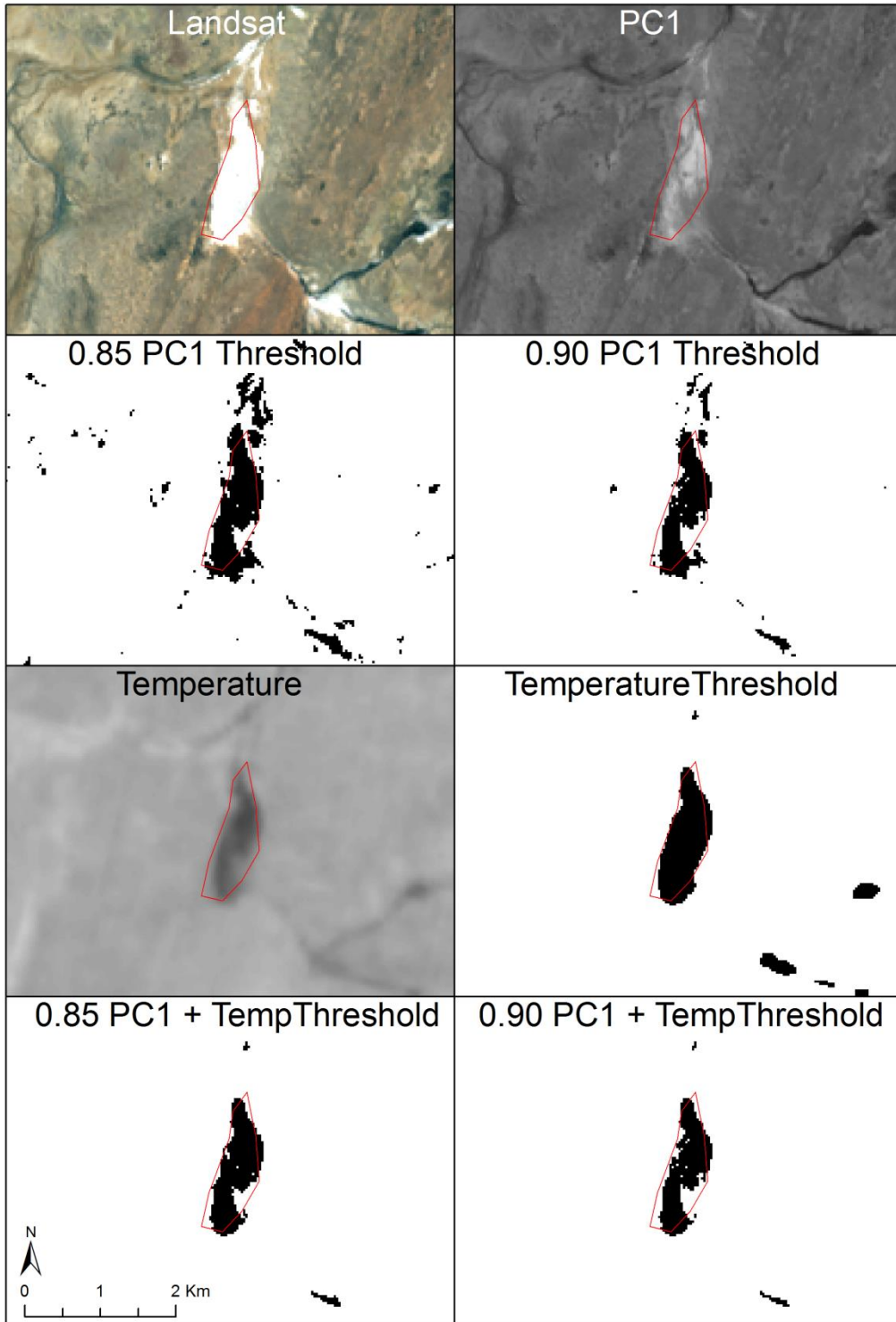
Gotch polygon 4



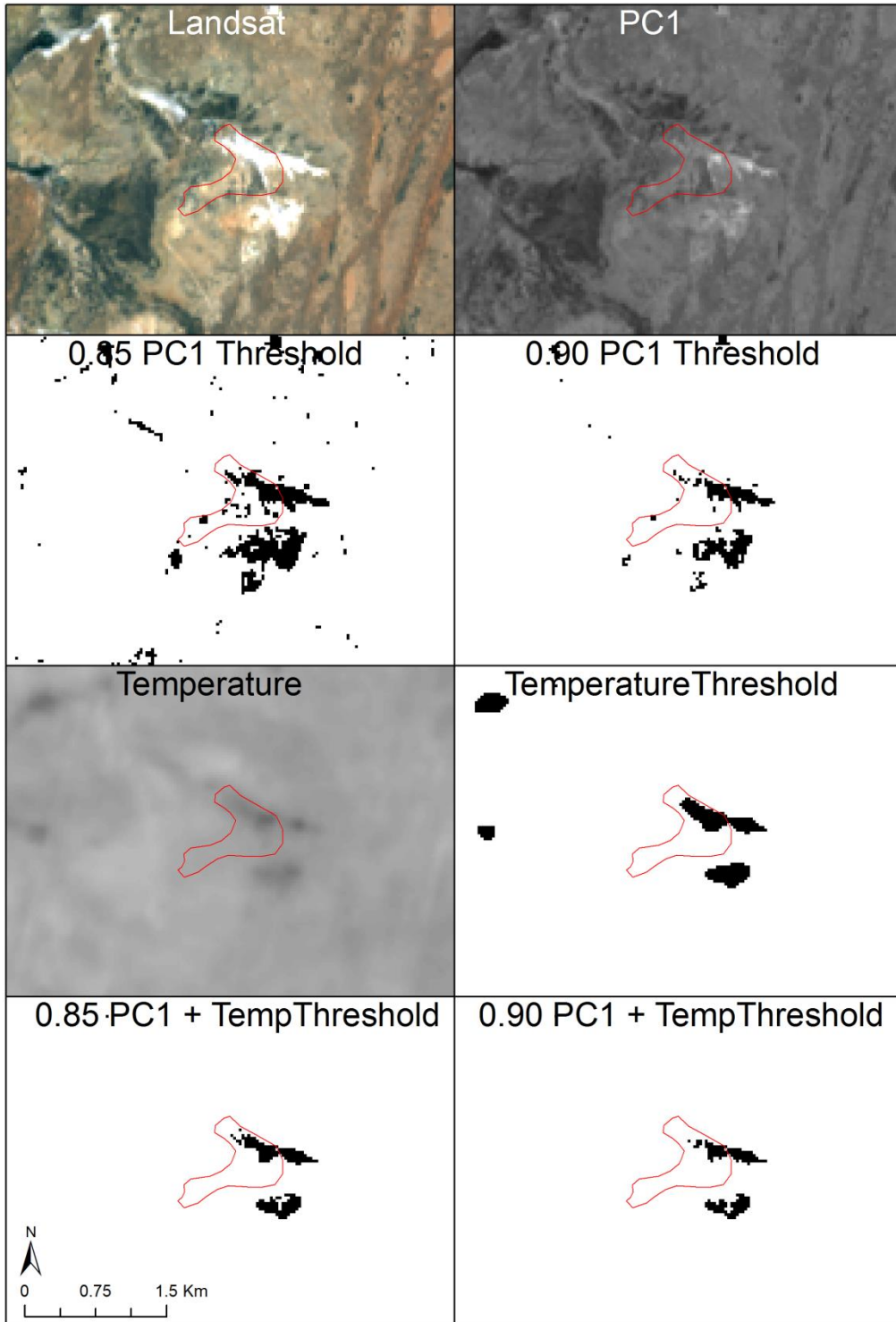
Gotch polygon 5



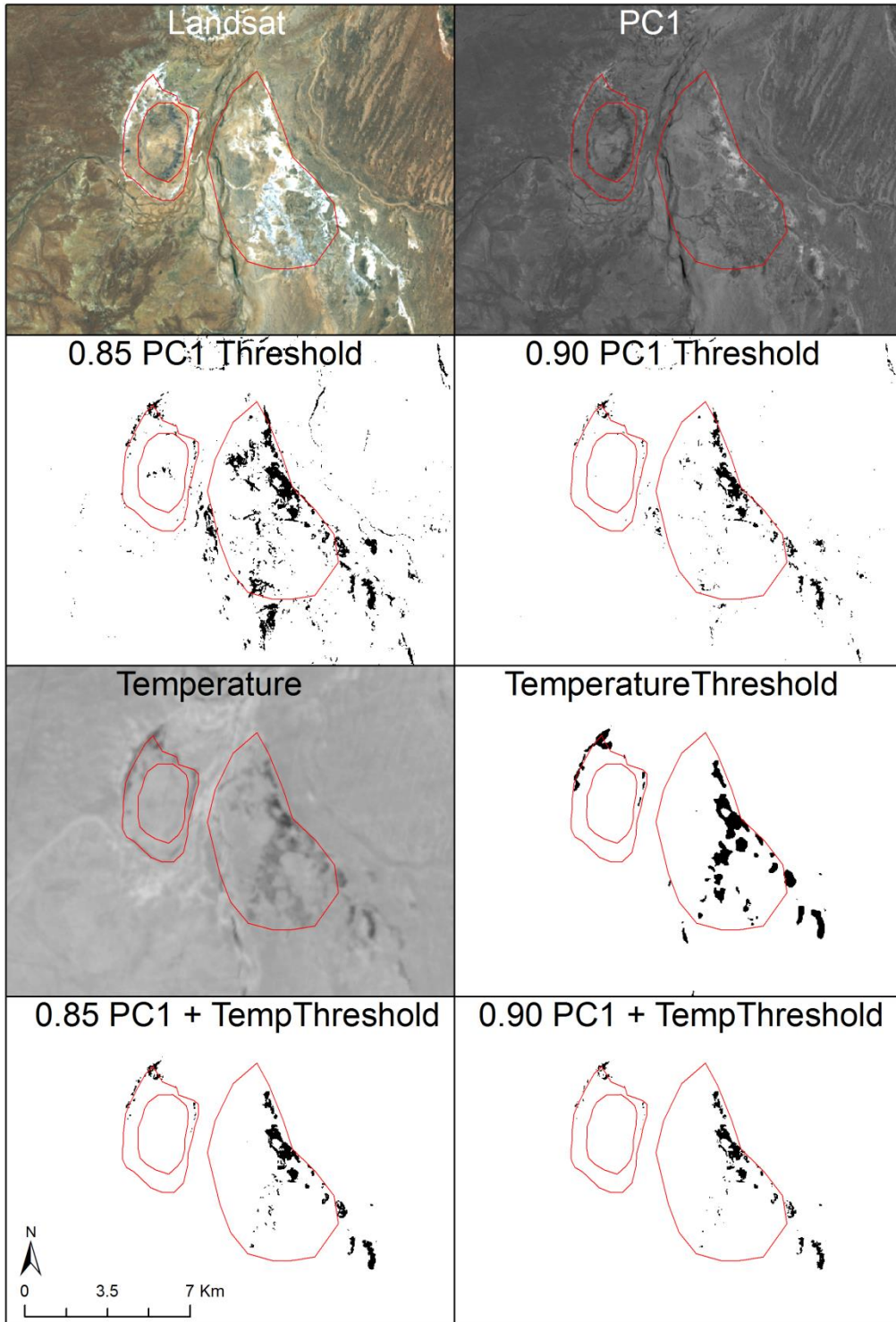
Gotch polygon 6



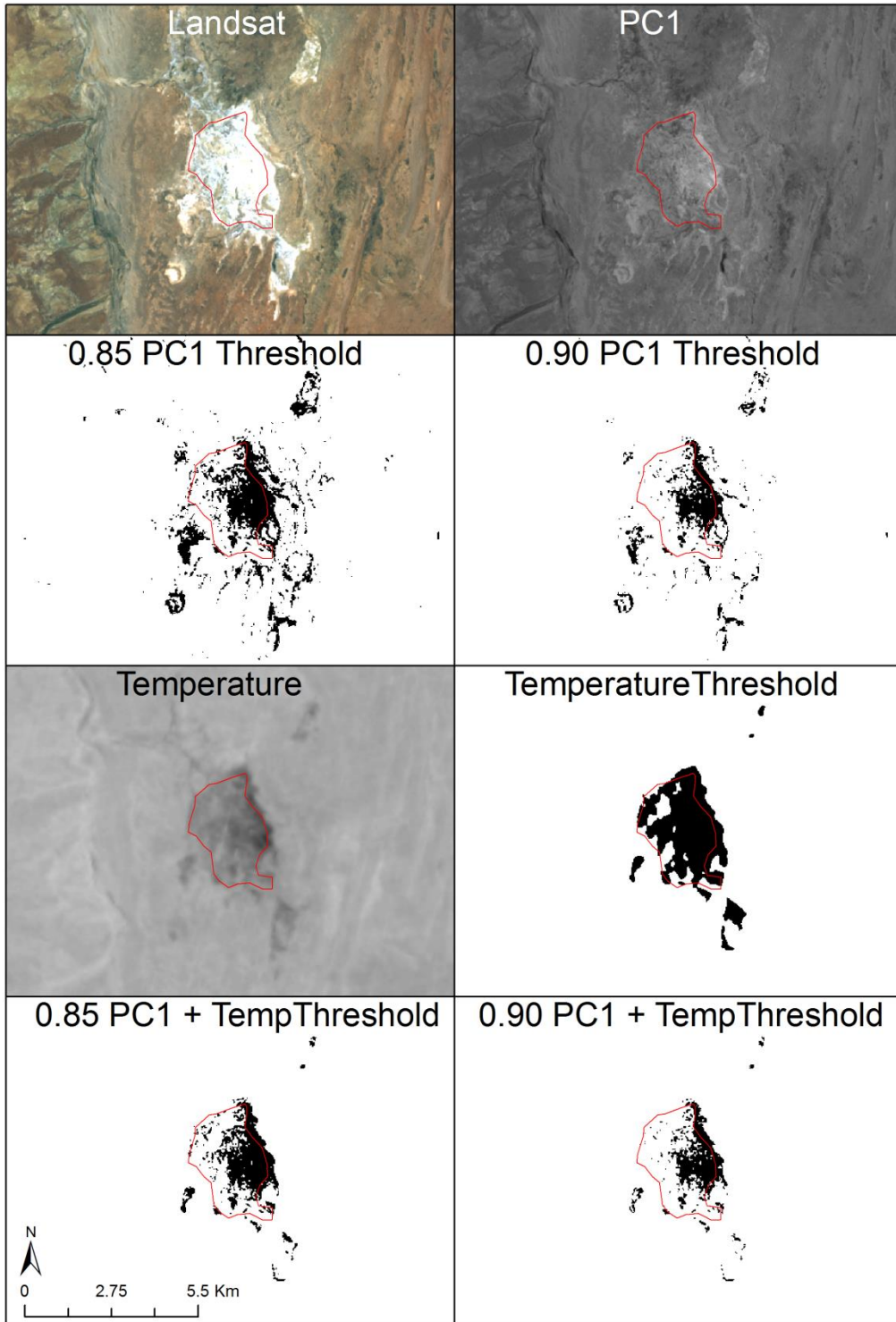
Gotch polygon 7



Gotch polygon 8



Gotch polygon 9 and 10



**Gotch polygon 11**